

# CSVQA: A Chinese Multimodal Benchmark for Evaluating STEM Reasoning Capabilities of VLMs

Ai Jian\*, Weijie Qiu\*, Xiaokun Wang, Peiyu Wang, Yunzhuo Hao,  
Jiangbo Pei, Yichen Wei, Yi Peng, Xuchen Song<sup>†</sup>

Skywork AI, Kunlun Inc.  
xuchen.song@kunlun-inc.com

## Abstract

Vision-Language Models (VLMs) have demonstrated remarkable progress in multimodal understanding, yet their capabilities for scientific reasoning remains inadequately assessed. Current multimodal benchmarks predominantly evaluate generic image comprehension or text-driven reasoning, lacking authentic scientific contexts that require domain-specific knowledge integration with visual evidence analysis. To fill this gap, we present CSVQA, a diagnostic multimodal benchmark specifically designed for evaluating scientific reasoning through domain-grounded visual question answering. Our benchmark features 1,378 carefully constructed question-answer pairs spanning diverse STEM disciplines, each demanding domain knowledge, integration of visual evidence, and higher-order reasoning. Compared to prior multimodal benchmarks, CSVQA places greater emphasis on real-world scientific content and complex reasoning. We additionally propose a rigorous evaluation protocol to systematically assess whether model predictions are substantiated by valid intermediate reasoning steps based on curated explanations. Our comprehensive evaluation of 15 VLMs on this benchmark reveals notable performance disparities, as even the top-ranked proprietary model attains only 49.6% accuracy. This empirical evidence underscores the pressing need for advancing scientific reasoning capabilities in VLMs. Our CSVQA is released at <https://huggingface.co/datasets/Skywork/CSVQA>.

## 1 Introduction

The emergence of large language models (LLMs) [1, 2, 3] has significantly advanced natural language understanding and generation, paving the way for vision-language models (VLMs) that integrate visual and textual modalities for robust multimodal reasoning [4, 5, 6, 7, 8]. As VLMs rapidly evolve, there is a growing need for multimodal benchmarks capable of rigorously evaluating their cross-modal comprehension and reasoning abilities.

While recent multimodal benchmarks have driven significant progress, they remain largely general-purpose, primarily focusing on everyday images and commonsense reasoning. State-of-the-art (SOTA) models such as InternVL2.5-78B [9] have achieved impressive results, scoring 95.1% on DocVQA [10], 84.1% on InfoVQA [11], and 88.3% on MMBench [12]. However, these benchmarks primarily assess perceptual understanding and fall short of rigorously evaluating the complex reasoning skills required in scientific domains.

In this work, we address the need for a comprehensive evaluation of scientific reasoning in VLMs by introducing CSVQA, a human-aligned multimodal benchmark in Chinese contexts specifically

\*Equal contribution

<sup>†</sup>Corresponding author

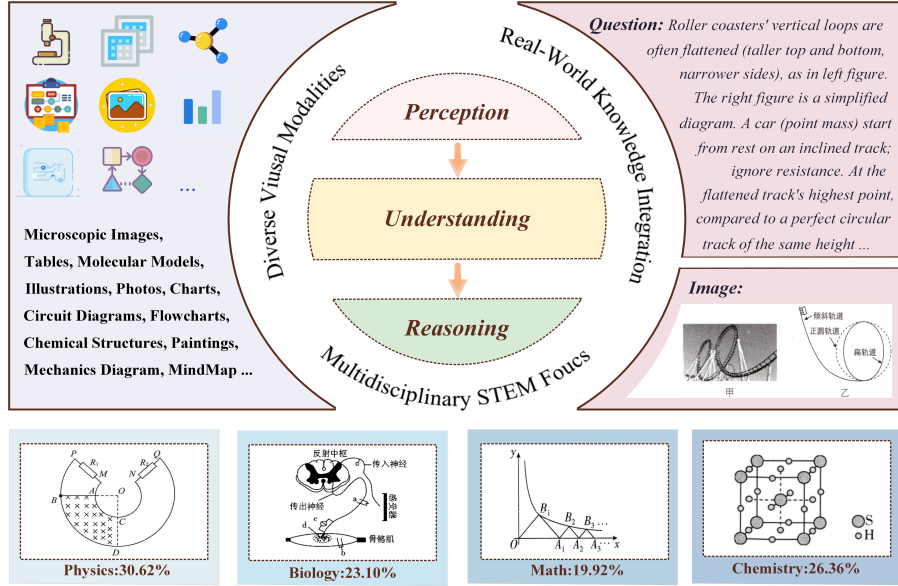


Figure 1: Challenges in the CSVQA Benchmark. (a) **Multidisciplinary STEM Focus**: Questions cover STEM subjects, ensuring comprehensive evaluation across disciplines; (b) **Diverse Visual Modalities**: The benchmark includes 14 types of images; (c) **Integration of Domain-Specific Knowledge and Real-World Scenarios**.

crafted. CSVQA is designed to evaluate the capability of VLMs to comprehend and reason about scientific content in images, moving beyond superficial pattern recognition to require integrated perception, understanding, and reasoning. Derived from authentic pedagogical materials across physics, chemistry, biology, and mathematics, the dataset comprises 1,378 rigorously validated problems with structured solution frameworks. It features a multimodal design that incorporates 14 types of scientific visual modalities, supporting both multiple-choice diagnostics and open-ended reasoning tasks, which fills a critical evaluation gap and offers a more demanding testbed for assessing advanced reasoning capabilities. Additionally, a challenging subset CSVQA-Hard is constructed based on difficulty scores and dependence on visual reasoning.

We evaluate 15 VLMs including both open-source and closed-source models on CSVQA and observe three key findings. These findings demonstrate that current VLMs still struggle with rigorous scientific reasoning:

- **Substantial Performance Gap.** The best-performing model, o1 [43], achieves only 49.6% overall accuracy, highlighting persistent domain-specific challenges where even SOTA models achieve sub-60% accuracy. In the meanwhile, Qwen-2.5-78B-Instruct attains 38.5% accuracy, the narrow gap between open-weight and proprietary systems revealing tangible progress in open model development, yet underscores the significant challenges in scientific visual reasoning faced by current models.
- **Modality Specific Weaknesses.** Models exhibit pronounced deficiencies in physics-related tasks, with a notable drop in accuracy, likely attributable to the abstract and symbolic nature of visual representations. Similarly, performance on open-ended questions is substantially lower, indicating difficulties in generating coherent reasoning without predefined options. On the CSVQA-hard subset, accuracy further declines, exposing limitations in handling complex scientific concepts and visual reasoning abilities.
- **Reasoning Demand.** Most models exhibit improved performance with Chain-of-Thought (CoT) prompting on our benchmark, indicating that the dataset comprises reasoning-intensive tasks requiring step-by-step logical inference. To rigorously evaluate reasoning ability while minimizing the influence of random guessing, we introduce process-tracing experiments. The further performance drop observed in certain models highlights the gap between superficial pattern recognition and genuine multimodal reasoning.

## 2 Related Work

**Vision-Language Models.** Recent advances in large-scale multimodal pretraining have aimed at unifying vision and language representations, significantly improving the performance of VLMs. Early methods, such as LXMERT [13] and UNITER [14], employed region-based features from object detectors and fused them with text encoders. More recent models like CLIP [15] and ALIGN [16] leverage large-scale image-text pairs sourced and use Vision Transformers to learn visual representations end-to-end. Encoder-free models [17, 18] present an alternative approach where visual and textual information are integrated into a shared embedding space, eliminating the need for separate encoders for each modality. More recently, cutting-edge models such as Gemini 2.0 [19] and o1 [43] have pushed the boundaries of multimodal reasoning by offering real-time perception, higher visual fidelity, and improved alignment across modalities.

**Commonsense VQA Benchmarks.** Visual Question Answering (VQA) is a widely studied task that requires an AI system to answer questions based on image content. Early VQA datasets focus primarily on object recognition and general visual question answering [21]. Subsequent developments introduced broader capabilities spanning optical character recognition (OCR) [10, 11, 22] and commonsense reasoning [12]. Knowledge-based VQA benchmarks have been proposed to push models beyond image content alone. OK-VQA [23] target questions that require external knowledge not evident in the image, such as world facts or commonsense. While these require integrating information beyond the visual, the knowledge is typically of a general nature and not specialized scientific reasoning.

**Multimodal Scientific Benchmarks.** Our work is closely related to benchmarks that combine images with scientific or educational question answering. One prominent example is ScienceQA [24], which contains multiple-choice science questions spanning topics in natural science, social science, and language science, primarily at the elementary and high school level. However, ScienceQA’s many questions can be answered by recalling facts or reading text in the associated diagram, rather than truly interpreting novel visual data. To evaluate more advanced and diverse skills, several recent benchmarks extend multimodal QA to higher levels. MMMU [25] is a benchmark with over 11k questions covering college-level knowledge across 30 subjects and EMMA [26] is designed to evaluate visual-relied reasoning, however both of them offering little insight into the reasoning process of models. Progress in scientific domains has been mostly limited to mathematics, as seen in MathVista [27] and MathVision [28]. In contrast, CSVQA offers naturally occurring multimodal questions in Chinese, spanning multiple disciplines and accompanied by high rates of detailed step-by-step explanations, thereby providing a new litmus test for the reasoning abilities of VLMs.

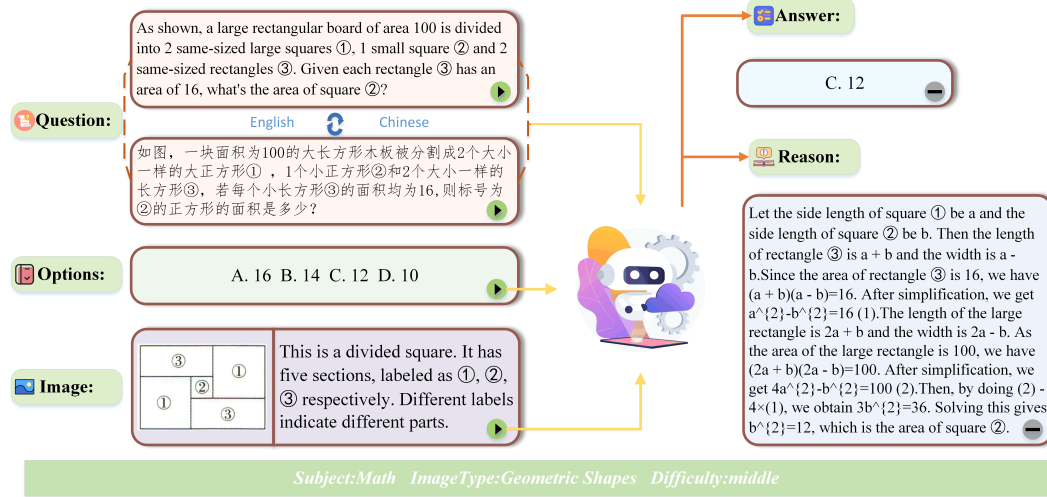


Figure 2: An example of a math problem from the CSVQA benchmark. Multi-step reasoning is required for solving the problem.

### 3 The CSVQA Benchmark

#### 3.1 Dataset Description

The Chinese STEM Visual Question Answering (CSVQA) benchmark establishes a rigorous multimodal evaluation framework specifically designed to quantify scientific reasoning capabilities in VLMs. Meanwhile, CSVQA introduces three key challenges that differentiate it from most existing benchmarks, as illustrated in Fig. 1. First, its coverage of multiple STEM disciplines which requires diverse domain knowledge and reasoning strategies. Second, the inclusion of 14 distinct visual modalities introduces significant variation in visual structure and complexity, testing a model’s ability to generalize across image types. Third, many questions are grounded in real-world scenarios and demand domain-specific knowledge, requiring models to go beyond pattern recognition and engage in context-aware reasoning.

An overview of the dataset’s composition is presented in Table 1. CSVQA contains 1,378 expert-annotated questions with moderate average length, balancing language processing load and reasoning depth. Nearly 81% of items is paired with a detailed explanation, which is particularly valuable for analyzing logical missteps in model predictions. Furthermore, we incorporated a bilingual dataset generated after translation, allowing for a broader range of test scenarios.

Fig. 3 demonstrates that CSVQA features a more uniform, extended, and balanced length distribution compared to existing benchmarks. This characteristic enables more robust evaluation of reasoning across varied input conditions while establishing a more challenging assessment framework. Moreover, the dataset maintains an equitable distribution of both question types and difficulty levels, effectively mitigating sampling bias.

As illustrated in Fig. 6, we utilized GPT-4o [20] to evaluate each question across image-text correlation, intrinsic difficulty, and reasoning complexity, subsequently categorizing them into three distinct difficulty levels. To specifically identify visually challenging questions, we implemented an additional filtering approach. We feed only the textual components to Gemini2.0-flash [19], Claude3.7-sonnet [29], Qwen2.5VL-78B-Instruct [30] and DeepSeekR1 [3], retaining those consistently answered incorrectly. The intersection of these visually dependent samples with previously classified hard questions formed our CSVQA-Hard subset.

Statistics	Number
Total Questions	1378
Image Types	14
Easy: Medium: Hard	22.6%:67.4%:10.0%
Multiple-choice Question	1278
Open Question	100
With an Explanation	81.1%
Image in the Question	1341
Image in Option	37
Average question length	69.7
Average option length	12.1
Average explanation length	123.5

Table 1: Key statistics of the CSVQA. To better compare with other datasets, the length analysis is conducted in English.

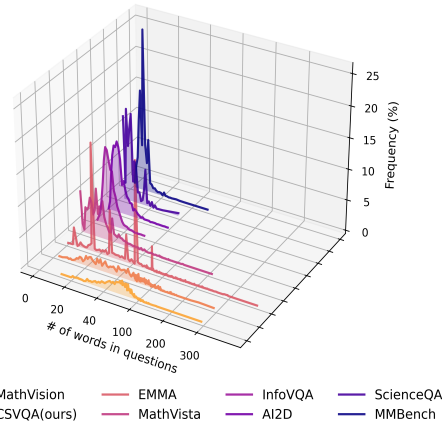


Figure 3: Question length distribution of related datasets.

#### 3.2 Dataset Collection

The dataset is sourced from publicly available Chinese high school textbooks and examination papers across STEM disciplines. To ensure high-quality alignment, we use a four-phase quality control pipeline, improving efficiency over traditional methods. The process begins by parsing source materials and applying OCR [31] to extract textual and visual data. Then we apply an automated alignment pipeline which is powered by DeepSeekV3 [32] to establish semantic correspondences



between questions and answers. Manual screening then addresses complex cases, such as multi-page layouts and mixed text-image formats. Finally, the benchmark undergoes three independent reviews: schema validation, integrity checks for completeness, and domain-specific audits with the help of annotators to ensure subject accuracy. From an initial pool of approximately 100,000 raw entries, we filtering out unsuitable question types like proof-based or diagram-drawing tasks, discarding samples without associated images, and removing mismatched question-answer pairs as flagged by the LLM, then we apply human curated subset of high-quality multimodal items is retained for the final dataset.

### 3.3 Comparisons with Existing Benchmarks

Benchmark	UniQ	I.S	I.T	AvgQ	Explanation	Subjects	Answer
ScienceQA	9,122	10,332	5	12.1	90.5%	STEM&Humanities (P.H)	MC
AI2D	4,563	4,903	diagram	9.8	✗	Science (P)	MC
OKVQA	14,055	14,031	photos	8.09	✗	General Knowledge	Open
MMMU	11,550	12,286	30	59.33	17.62%	STEM&Humanities (U)	MC&Open
MathVista	4,746	5487	-	15.6	✗	Math-focused	MC&Open
EMMA	2,788	-	-	55.2	✗	STEM&code	MC&Open
CSVQA	1,378	1,378	14	69.7	81.1%	STEM-focused (H)	MC&Open

Table 2: Comparisons with existing benchmarks. UniQ: number of unique questions; I.S: number of images; I.T: number of image types; AvgQ: average question length; MC: multiple-choice; "-" not mentioned; P/H/U denote primary school/high school/university levels.

In this section, we compare CSVQA with existing benchmarks in Table 2. The selected datasets were chosen for their relevance to specific areas: ScienceQA [24], EMMA[26] MathVista [27] focus on STEM reasoning; AI2D [21] emphasizes visual-text alignment in school contexts; and MMMU [25] provides a broad cross-domain evaluation.

CSVQA distinguishes itself from existing benchmarks through several critical aspects. Firstly, it maintains a *pure STEM focus*. Unlike ScienceQA and MMMU, which include substantial non-STEM content, CSVQA maintains rigorous focus on four core scientific disciplines, ensuring all questions directly assess STEM competencies. Another significant differentiator is CSVQA’s *explanation-driven design*. CSVQA features comprehensive solution breakdowns accompanying 81.1% questions, which is crucial for diagnosing reasoning failures and improving model interpretability. CSVQA places a strong emphasis on *reasoning intensive tasks* by featuring 14 specialized visual formats and long, information-rich questions averaging 69.7 words, collectively pushing models toward deeper understanding of domain-specific scientific representations. Finally, by using native Chinese STEM terminology and notation, CSVQA ensures *linguistic and cultural authenticity*, setting it apart from translated benchmarks that may lose nuance in adaptation.

## 4 Experiments

All experiments were conducted using NVIDIA H100 GPUs. To improve inference efficiency, we utilized VLLM [33], a high-performance inference framework, which accelerates text generation while preserving output quality. To ensure consistency across different models, we designed and provided a unified set of prompts specifically tailored for CSVQA. The inference process was automated through a dedicated script based on VLLM, supporting batch processing and ensuring reproducibility of results.

### 4.1 Experiment setups

**Baselines.** (i) Fuyu-8B [34] directly projects image patches into the Transformer’s first layer. (ii) Mono-InternVL [18] combines visual experts with a fixed LLM through multimodal mixture-of-experts integration. (iii) Phi-4 [35] integrates multimodal inputs using LoRA adapters and modality-specific routing. (iv) DeepSeek-VL2 [36] is a Mixture-of-Experts VLM with dynamic tiling for high-resolution image encoding and uses compressed key-value caches. (v) Gemma 3 [37] features broader multilingual support and efficient long-context processing. (vi) InternVL3 [38] builds upon InternVL2.5 [9] addressing alignment challenges in post-hoc adaptation while introducing

improvements such as variable visual position encoding. (vii) Idefics3 [39] improves document understanding over its predecessor by introducing a new visual tokenization scheme and expanding data. (viii) LLaVA-1.5 [40] enhances visual instruction tuning by aligning CLIP-based vision features. (ix) Pixtral [41] uses a from-scratch vision encoder with hierarchical attention to tokenize full-resolution images within a 128K-token context. (x) Qwen2.5VL-Instruct [30] and QVQ [42], released by the Qwen team, are high-performing models evaluated across standard benchmarks. (xi) We further include closed-source upper bounds by evaluating Claude3.7-sonnet [29], GPT-4o [8], Gemini2.0-flash [19], and o1 [43] to contextualize performance.

**Evaluations.** To establish a performance floor, a Random Choice baseline is included, which selects one or more answers uniformly from the answer options. For multiple-choice questions, models are constrained to follow a fixed response format using rule-based protocols, with answers extracted via a deterministic parser. Notably, while questions may have single or multiple correct answers, models receive no explicit indication of the number of valid options. If the parser fails due to format violations, we employ a fallback mechanism using GPT-4o [8] to match the answers. Open-ended questions are scored only by GPT-4o to ensure consistency and accuracy of scoring.

## 4.2 Results

**Overall Performance Analysis.** Table 3 shows that the best-performing model on CSVQA is the closed-source o1, achieving an overall accuracy of 49.6%. Among open-source models, Qwen2.5VL-78B leads with 38.5% accuracy, followed closely by InternVL3-78B at 37.4% and QVQ-72B at 36.6%. In contrast, lightweight models score near or below 10%, indicating significant limitations in handling scientific visual reasoning tasks. In the meanwhile, open-ended questions remain challenging across the board, with most models scoring noticeably lower compared to multiple-choice formats.

**Open-Source vs. Closed-Source.** Overall, closed-source models consistently outperform their open-source counterparts across all evaluation dimensions. The strongest closed-source model surpasses the best-performing open-source model by a margin of 11.1% in overall accuracy. This advantage extends to individual subject areas, with particularly notable differences observed in Math and Physics. The performance gap suggests that closed-source models possess superior capabilities in handling both numerical reasoning and visual understanding tasks.

Model	Overall	Biology	Chemistry	Math	Physics	Open	MC
Random Choice	5.2	5.1	6.2	4.5	5.7	0	5.7
<b>Open-source VLM</b>							
Fuyu-8B [34]	4.9	6.3	5.6	3.5	4.3	2.0	5.1
Deepseek-VL2 [36]	6.2	7.0	6.2	7.6	4.5	8.0	6.0
LLaVA1.5-13B [40]	7.5	10.7	9.4	5.4	5.5	4.0	7.8
MonoInternVL [18]	9.3	7.3	9.1	9.2	10.9	3.0	9.8
Idefics3-8b [39]	10.1	11.7	15.2	7.0	7.1	4.0	10.6
Pixtral-12B [41]	10.5	15.3	8.8	8.6	10.0	5.0	10.9
Phi-4 [35]	11.5	13.3	16.1	8.9	8.3	7.0	11.8
Gemma3-27B [37]	22.9	26.0	23.5	27.0	17.1	23.0	22.9
Internvl2-5-78B [9]	28.4	36.3	36.1	24.1	19.7	16.0	29.3
QVQ-72B [42]	36.6	40.7	41.3	33.7	32.0	32.0	36.9
Internvl3-78B [38]	37.4	<b>46.0</b>	41.1	36.5	28.9	30.0	38.0
Qwen2.5VL-72B [30]	38.5	45.7	40.8	37.5	32.2	29.0	39.2
<b>Closed-source VLM</b>							
GPT-4o [20]	23.6	28.0	23.5	23.5	20.6	18.0	24.0
Claude3.7 [29]	36.6	41.7	38.1	37.1	31.3	32.0	36.9
Gemini2.0-flash [19]	<b>44.1</b>	45.0	<b>45.5</b>	<b>47.6</b>	<b>39.8</b>	<b>46.0</b>	<b>44.0</b>
o1 [43]	<b>49.6</b>	<b>46.2</b>	<b>45.1</b>	<b>59.0</b>	<b>49.1</b>	<b>41.3</b>	<b>50.2</b>

Table 3: Accuracy of CSVQA Model Evaluation. We highlight the top two performers across all models in each column. The best-performing model in each column is **underlined and bolded**, and the second-best is **bolded**. We use Qwen2.5VL-72B (short for Qwen2.5VL-78B-Instruct) in our experiments for consistent formatting.

## 5 Analysis

### 5.1 Insights from Dataset Statistics

**Performance Between Disciplines.** The performance of VLMs exhibits substantial variation across scientific disciplines, reflecting the distinct cognitive demands of each subject. Compared to Physics and Math, which emphasize logical reasoning and analytical problem solving, Biology and Chemistry rely more heavily on domain-specific knowledge. This distinction helps explain the widespread underperformance of most models in Physics and Math, as shown in Fig. 4. In contrast, Gemini2.0-flash and o1 exhibit comparatively strong performance in these subjects, suggesting more advanced reasoning and generative abilities.

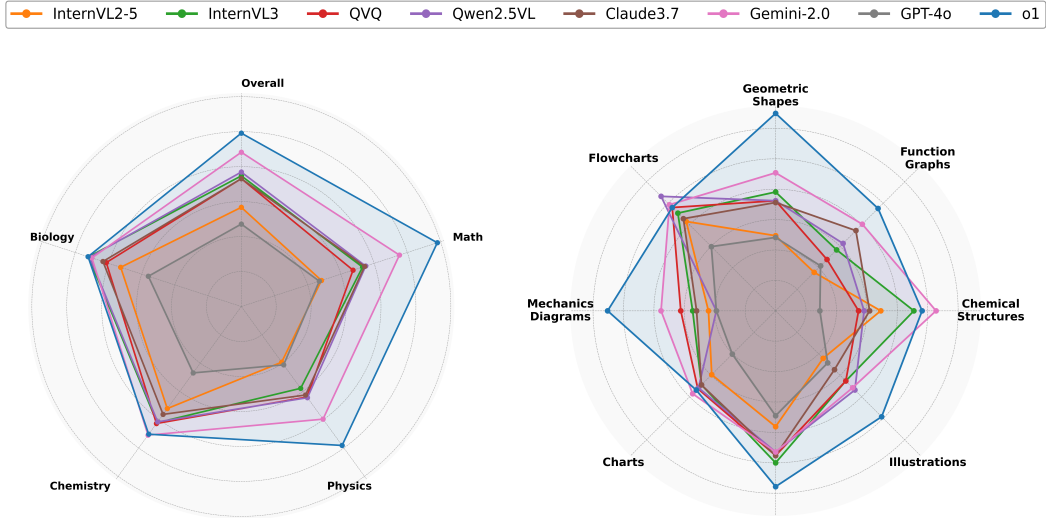


Figure 4: Subject accuracy comparison across models. Model names are abbreviated in the figures of Section 5 for visual clarity.

Figure 5: Different visual modalities accuracy across models .

**Impact of Visual Modalities.** As shown in Fig. 5, models tend to perform well on text-rich or structured images, such as flowcharts and tables, which present large amounts of directly accessible information through their visual layout, as well as on low-content symbolic images, such as chemical structures, where much of the necessary information is provided in the accompanying question. In these cases, the image functions primarily as a visual reference rather than a source requiring complex reasoning. In contrast, performance degrades on image types that demand deeper visual understanding or more intricate perception.

**Performance Across Difficulty Levels.** As illustrated in Fig. 7, models generally demonstrate high accuracy on easy and medium questions. However, they suffer a noticeable performance drop on the hard subset. Interestingly, even the top-performing models, those who excel in overall accuracy have shown significantly reduced effectiveness on hard questions. This performance gap highlights the limitations of current VLMs in handling samples with high visual dependency and complex reasoning requirements. Furthermore, these results validate our difficulty classification methodology while highlighting the need for more advanced visual perception and reasoning capabilities to address genuinely challenging multimodal tasks.

### 5.2 Explanation-Driven Evaluation.

To determine whether correct answers stem from valid reasoning rather than random guessing or spurious correlations, we conduct an explanation-driven evaluation. We first extract a subset of correctly answered questions containing human-annotated solution steps. For each case, we employ GPT-4o to assess whether the models’ response aligns with the step-by-step explanation provided by annotation, evaluating the validity of the underlying reasoning process, which enables us to identify instances where models arrived at correct answers without genuine understanding.

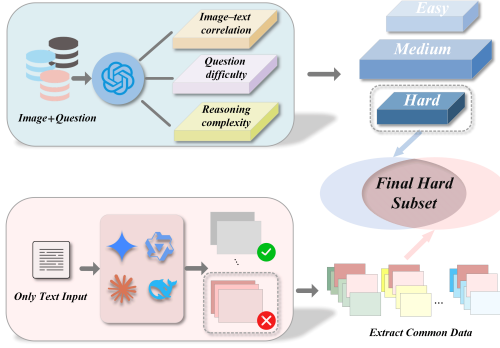


Figure 6: Pipeline for constructing the CSVQA-Hard via the intersection of difficulty and visual dependency filtering.

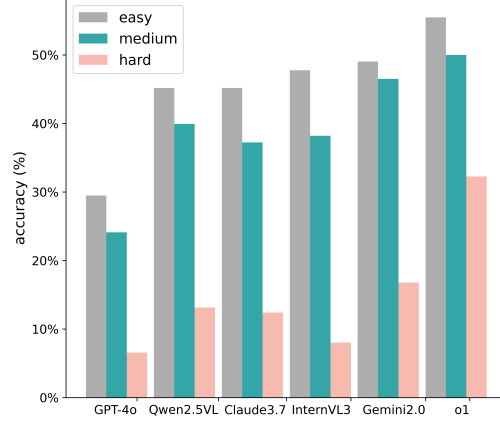


Figure 7: Model performance comparison across different difficulty levels.

Table 4 presents the alignment accuracy across six high-performing models, with gray parenthetical values indicating the number of evaluated instances per model. Although all responses were factually correct, we find significant variation in reasoning consistency. For instance, o1 demonstrates strong alignment at 95.4%, while Qwen2.5VL-72B and InternVL3-78B show substantially lower consistency with 67.6% and 74.9%, respectively. The marked difference between closed-source and open-source models suggests that the latter are more inclined to arrive at correct answers through pattern matching or memorization rather than genuine logical reasoning. Additionally, we observe that most models tend to achieve higher accuracy on open-ended formats. The observed pattern derives from the open-ended format’s dual mechanism of inherently reducing guesswork incidence through probabilistic constraints, while simultaneously enhancing cognitive focus by eliminating predefined answer options.

Model	Overall Open MC		
QVQ-72B(404)	67.6	75.0	67.3
InternVL3-78b(411)	74.9	91.7	74.6
Qwen2.5VL-72B(427)	80.8	78.6	80.9
Gemini2.0-flash(492)	80.9	87.5	80.6
Claude3.7-sonnet(407)	90.7	87.5	90.8
o1(521)	95.4	100	95.2

Table 4: Accuracy of explanation-aligned responses on correctly answered questions. Gray values indicate the total number of extracted instances per model.

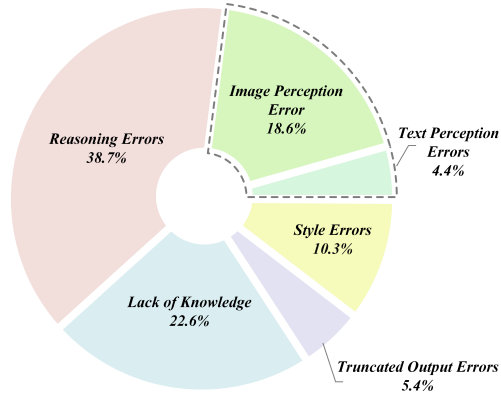


Figure 8: Error distribution.

### 5.3 Error Analysis

To gain deeper insight into the reasoning failures of current VLMs, we randomly sampled 180 questions that Claude3.7-sonnet answered incorrectly and conducted a manual categorization of failure modes, as shown in Fig.8. Detailed example cases are provided in the supplementary material. The results are summarized as follows.

**Perception errors (23.0%)** arise from inaccurate interpretation of either textual or visual input, with visual errors occurring more frequently, reflecting difficulties in processing complex graphical information. In terms of textual perception, models often substitute key conditions with incorrect values or overlook them altogether. Visual perception errors commonly involve miscounting objects or

misidentifying shaded areas. **Reasoning errors (38.7%)** arise when the model correctly interprets the input but fails to produce accurate answers due to flawed logical reasoning. Common issues include incorrect arithmetic operations, misapplication of scientific rules, and inconsistencies across different stages of inference. **Lack of knowledge (22.6%)** reflects an insufficient understanding of domain-specific concepts. Models may misinterpret technical terminology or fail to apply foundational scientific principles correctly. **Other errors (15.7%)** primarily fall into two categories. First, truncated outputs occur when the model exceeds token limitations, often resulting in incomplete or repetitive responses. Second, style-related errors involve the model responding in English despite Chinese prompts, a failure mode frequently accompanied by reasoning deficiencies.

#### 5.4 Does CoT help?

To evaluate the impact of explicit reasoning guidance, we compare model performance with and without CoT prompting. As shown in Table 5, the effects of CoT are mixed and highly model-dependent. Certain models are excluded due to their generation embedding reasoning traces. The results indicate that CoT prompting does not universally improve performance. While certain light models show notable gains which up to 6.5%, most advanced models experience a performance drop, suggesting that these models may already possess sufficient internal reasoning capabilities. For instance, Gemini2.0-flash show significant decreases of 11.8% in overall accuracy, with open-format accuracy dropping by as much as 23.0%.

It can be concluded that the effectiveness of CoT prompting varies by model architecture and question type. Lightweight or instruction-tuned models may benefit from guided reasoning steps, whereas stronger models may already encode internal reasoning capabilities that can be disrupted by rigid directly output templates, especially in open-ended questions.

Model	Overall	Biology	Chemistry	Math	Physics	Open	MC
Phi-4	4.8(↓6.7)	4.0	3.5	4.4	6.6	3.0(↓4.0)	4.9(↓6.9)
Pixtral-12B	8.2(↓2.3)	14.7	6.7	4.8	7.3	1.0(↓4.0)	8.8(↓2.2)
Deepseek-VL2	12.7(↑6.5)	13.0	11.4	14.9	11.8	3.0(↓5.0)	13.5(↑7.4)
LLaVA1.5-13B	13.6(↑6.0)	14.7	16.7	14.0	10.0	2.0(↓2.0)	14.5(↑6.7)
Idefics3-8B	13.8(↑3.7)	16.0	16.4	10.8	12.3	4.0(-)	14.5(↑4.0)
Gemma3-27B	18.1(↓4.8)	21.3	15.8	24.1	13.0	12.0(↓11.0)	18.5(↓4.3)
InternVL2-5-78B	30.6(↑2.3)	39.7	37.5	29.2	19.7	18.0(↑2.0)	31.6(↑2.3)
InternVL3-78b	32.4(↓5.0)	42.0	38.4	29.8	22.5	15.0(↓15.0)	33.7(↓4.2)
Qwen2.5VL-72B	37.3(↓1.2)	52.7	42.8	28.6	28.4	16.0(↓13.0)	39.0(↓0.2)
GPT-4o	19.7(↓3.8)	30.0	18.8	19.7	13.3	8.0(↓10.0)	20.7(↓3.4)
Gemini2.0-flash	32.3(↓11.8)	43.7	30.2	35.2	23.7	23.0(↓23.0)	33.0(↓11.0)

Table 5: Accuracy without CoT prompting. Values in parentheses indicate the change in accuracy compared to direct answer generation (↑ improvement, ↓ degradation).

## 6 Conclusion

We have presented CSVQA, a new multimodal benchmark specifically aimed at evaluating and advancing the scientific reasoning capabilities of vision-language models. In constructing CSVQA, we placed a strong emphasis on question quality, diversity, and the need for genuine reasoning, resulting in a benchmark that pushes models far beyond the comfort zone of general image understanding. Our systematic evaluation demonstrates that while models perform adequately in text-heavy domains, they exhibit significant weaknesses in visually grounded and abstract reasoning tasks. Performance declines further on questions requiring deeper inference or strong visual dependency, as evidenced by the CSVQA-hard subset. We also explore the effect of CoT prompting, finding that it enhances performance for most models. Additionally, we introduce explanation-driven evaluation to assess whether model predictions align with valid reasoning processes. In summary, CSVQA establishes a new standard for assessing scientific reasoning in complex multimodal settings. We anticipate that this benchmark will advance the development of more reliable, interpretable, and educationally aligned VLMs.



## References

- [1] OpenAI. Gpt-4 technical report, 2023. 1
- [2] Hugo Touvron, Louis Martin, Kevin Stone, Peter Albert, Amjad Almahairi, Yasmine Babaei, Nikolay Bashlykov, Soumya Batra, Prajjwal Bhargava, Shruti Bhosale, Dan Bikel, Lukas Blecher, Cristian Canton Ferrer, Moya Chen, Guillem Cucurull, David Esiobu, Jude Fernandes, Jeremy Fu, Wenyin Fu, Brian Fuller, Cynthia Gao, Vedanuj Goswami, Naman Goyal, Anthony Hartshorn, Saghar Hosseini, Rui Hou, Hakan Inan, Marcin Kardas, Viktor Kerkez, Madian Khabsa, Isabel Kloumann, Artem Korenev, Punit Singh Koura, Marie-Anne Lachaux, Thibaut Lavril, Jenya Lee, Diana Liskovich, Yinghai Lu, Yuning Mao, Xavier Martinet, Todor Mihaylov, Pushkar Mishra, Igor Molybog, Yixin Nie, Andrew Poulton, Jeremy Reizenstein, Rashi Rungta, Kalyan Saladi, Alan Schelten, Ruan Silva, Eric Michael Smith, Ranjan Subramanian, Xiaoqing Ellen Tan, Binh Tang, Ross Taylor, Adina Williams, Jian Xiang Kuan, Puxin Xu, Zheng Yan, Iliyan Zarov, Yuchen Zhang, Angela Fan, Melanie Kambadur, Sharan Narang, Aurelien Rodriguez, Robert Stojnic, Sergey Edunov, and Thomas Scialom. Llama 2: Open foundation and fine-tuned chat models, 2023. 1
- [3] DeepSeek-AI. Deepseek-r1: Incentivizing reasoning capability in llms via reinforcement learning, 2025. 1, 4
- [4] Peng Wang, Shuai Bai, Sinan Tan, Shijie Wang, Zhihao Fan, Jinze Bai, Keqin Chen, Xuejing Liu, Jialin Wang, Wenbin Ge, Yang Fan, Kai Dang, Mengfei Du, Xuancheng Ren, Rui Men, Dayiheng Liu, Chang Zhou, Jingren Zhou, and Junyang Lin. Qwen2-vl: Enhancing vision-language model’s perception of the world at any resolution. *arXiv preprint arXiv:2409.12191*, 2024. 1
- [5] Zhe Chen, Jiannan Wu, Wenhai Wang, Weijie Su, Guo Chen, Sen Xing, Zhong Muyan, Qinglong Zhang, Xizhou Zhu, Lewei Lu, et al. Internvl: Scaling up vision foundation models and aligning for generic visual-linguistic tasks. *arXiv preprint arXiv:2312.14238*, 2023. 1
- [6] Kimi Team. Kimi k1.5: Scaling reinforcement learning with llms, 2025. 1
- [7] Gemini Team. Gemini: A family of highly capable multimodal models, 2024. 1
- [8] OpenAI. Hello gpt-4o, 2024. 1, 6
- [9] Zhe Chen, Weiyun Wang, Yue Cao, Yangzhou Liu, Zhangwei Gao, Erfei Cui, Jinguo Zhu, Shenglong Ye, Hao Tian, Zhaoyang Liu, Lixin Gu, Xuehui Wang, Qingyun Li, Yimin Ren, Zixuan Chen, Jiapeng Luo, Jiahao Wang, Tan Jiang, Bo Wang, Conghui He, Botian Shi, Xingcheng Zhang, Han Lv, Yi Wang, Wenqi Shao, Pei Chu, Zhongying Tu, Tong He, Zhiyong Wu, Huipeng Deng, Jiaye Ge, Kai Chen, Kaipeng Zhang, Limin Wang, Min Dou, Lewei Lu, Xizhou Zhu, Tong Lu, Dahua Lin, Yu Qiao, Jifeng Dai, and Wenhai Wang. Expanding performance boundaries of open-source multimodal models with model, data, and test-time scaling, 2025. 1, 5, 6
- [10] Minesh Mathew, Dimosthenis Karatzas, and C. V. Jawahar. Docvqa: A dataset for vqa on document images, 2021. 1, 3
- [11] Minesh Mathew, Viraj Bagal, Rubèn Pérez Tito, Dimosthenis Karatzas, Ernest Valveny, and C. V. Jawahar. Infographicvqa, 2021. 1, 3
- [12] Yuan Liu, Haodong Duan, Yuanhan Zhang, Bo Li, Songyang Zhang, Wangbo Zhao, Yike Yuan, Jiaqi Wang, Conghui He, Ziwei Liu, Kai Chen, and Dahua Lin. Mmbench: Is your multi-modal model an all-around player?, 2024. 1, 3
- [13] Hao Tan and Mohit Bansal. Lxmert: Learning cross-modality encoder representations from transformers, 2019. 3
- [14] Yen-Chun Chen, Linjie Li, Licheng Yu, Ahmed El Kholy, Faisal Ahmed, Zhe Gan, Yu Cheng, and Jingjing Liu. Uniter: Universal image-text representation learning, 2020. 3

- [15] Alec Radford, Jong Wook Kim, Chris Hallacy, Aditya Ramesh, Gabriel Goh, Sandhini Agarwal, Girish Sastry, Amanda Askell, Pamela Mishkin, Jack Clark, Gretchen Krueger, and Ilya Sutskever. Learning transferable visual models from natural language supervision, 2021. 3
- [16] Chao Jia, Yinfei Yang, Ye Xia, Yi-Ting Chen, Zarana Parekh, Hieu Pham, Quoc V. Le, Yunhsuan Sung, Zhen Li, and Tom Duerig. Scaling up visual and vision-language representation learning with noisy text supervision, 2021. 3
- [17] Haiwen Diao, Xiaotong Li, Yufeng Cui, Yueze Wang, Haoze Deng, Ting Pan, Wenxuan Wang, Huchuan Lu, and Xinlong Wang. Evev2: Improved baselines for encoder-free vision-language models, 2025. 3
- [18] Gen Luo, Xue Yang, Wenhan Dou, Zhaokai Wang, Jiawen Liu, Jifeng Dai, Yu Qiao, and Xizhou Zhu. Mono-intervl: Pushing the boundaries of monolithic multimodal large language models with endogenous visual pre-training, 2025. 3, 5, 6
- [19] Google DeepMind. Introducing Gemini 2.0: Our New AI Model for the Agentic Era. <https://blog.google/technology/google-deepmind/google-gemini-ai-update-december-2024/>, 2024. 3, 4, 6
- [20] OpenAI. Gpt-4o system card, 2024. 4, 6
- [21] Aniruddha Kembhavi, Mike Salvato, Eric Kolve, Minjoon Seo, Hannaneh Hajishirzi, and Ali Farhadi. A diagram is worth a dozen images, 2016. 3, 5
- [22] Anand Mishra, Shashank Shekhar, Ajeet Kumar Singh, and Anirban Chakraborty. Ocr-vqa: Visual question answering by reading text in images. In *2019 International Conference on Document Analysis and Recognition (ICDAR)*, pages 947–952, 2019. 3
- [23] Kenneth Marino, Mohammad Rastegari, Ali Farhadi, and Roozbeh Mottaghi. Ok-vqa: A visual question answering benchmark requiring external knowledge, 2019. 3
- [24] Pan Lu, Swaroop Mishra, Tony Xia, Liang Qiu, Kai-Wei Chang, Song-Chun Zhu, Oyvind Tafjord, Peter Clark, and Ashwin Kalyan. Learn to explain: Multimodal reasoning via thought chains for science question answering, 2022. 3, 5
- [25] Xiang Yue, Yuansheng Ni, Kai Zhang, Tianyu Zheng, Ruoqi Liu, Ge Zhang, Samuel Stevens, Dongfu Jiang, Weiming Ren, Yuxuan Sun, Cong Wei, Botao Yu, Ruibin Yuan, Renliang Sun, Ming Yin, Boyuan Zheng, Zhenzhu Yang, Yibo Liu, Wenhao Huang, Huan Sun, Yu Su, and Wenhui Chen. Mmmu: A massive multi-discipline multimodal understanding and reasoning benchmark for expert agi, 2024. 3, 5
- [26] Yunzhuo Hao, Jiawei Gu, Huichen Will Wang, Linjie Li, Zhengyuan Yang, Lijuan Wang, and Yu Cheng. Can mllms reason in multimodality? emma: An enhanced multimodal reasoning benchmark. *arXiv preprint arXiv:2501.05444*, 2025. 3, 5
- [27] Pan Lu, Hritik Bansal, Tony Xia, Jiacheng Liu, Chunyuan Li, Hannaneh Hajishirzi, Hao Cheng, Kai-Wei Chang, Michel Galley, and Jianfeng Gao. Mathvista: Evaluating mathematical reasoning of foundation models in visual contexts, 2024. 3, 5
- [28] Ke Wang, Juntao Pan, Weikang Shi, Zimu Lu, Mingjie Zhan, and Hongsheng Li. Measuring multimodal mathematical reasoning with math-vision dataset, 2024. 3
- [29] Anthropic. Claude-3.7, 2025. 4, 6
- [30] Qwen Team. Qwen2.5 technical report, 2025. 4, 6
- [31] Bin Wang, Chao Xu, Xiaomeng Zhao, Linke Ouyang, Fan Wu, Zhiyuan Zhao, Rui Xu, Kaiwen Liu, Yuan Qu, Fukai Shang, Bo Zhang, Liqun Wei, Zhihao Sui, Wei Li, Botian Shi, Yu Qiao, Dahua Lin, and Conghui He. Mineru: An open-source solution for precise document content extraction, 2024. 4
- [32] DeepSeek-AI. Deepseek-v3 technical report. 4

- [33] Woosuk Kwon, Zhuohan Li, Siyuan Zhuang, Ying Sheng, Lianmin Zheng, Cody Hao Yu, Joseph E. Gonzalez, Hao Zhang, and Ion Stoica. Efficient memory management for large language model serving with pagedattention, 2023. 5
- [34] Rohan Bavishi, Erich Elsen, Curtis Hawthorne, Maxwell Nye, Augustus Odena, Arushi Somani, and Sağnak Taşirlar. Introducing our multimodal models, 2023. 5, 6
- [35] Microsoft. Phi-4-mini technical report: Compact yet powerful multimodal language models via mixture-of-loras. 5, 6
- [36] Zhiyu Wu, Xiaokang Chen, Zizheng Pan, Xingchao Liu, Wen Liu, Damai Dai, Huazuo Gao, Yiyang Ma, Chengyue Wu, Bingxuan Wang, Zhenda Xie, Yu Wu, Kai Hu, Jiawei Wang, Yaofeng Sun, Yukun Li, Yishi Piao, Kang Guan, Aixin Liu, Xin Xie, Yuxiang You, Kai Dong, Xingkai Yu, Haowei Zhang, Liang Zhao, Yisong Wang, and Chong Ruan. Deepseek-vl2: Mixture-of-experts vision-language models for advanced multimodal understanding, 2024. 5, 6
- [37] Gemma Team. Gemma 3. 2025. 5, 6
- [38] Jinguo Zhu, Weiyun Wang, Zhe Chen, Zhaoyang Liu, Shenglong Ye, Lixin Gu, Hao Tian, Yuchen Duan, Weijie Su, Jie Shao, Zhangwei Gao, Erfei Cui, Xuehui Wang, Yue Cao, Yangzhou Liu, Xingguang Wei, Hongjie Zhang, Haomin Wang, Weiye Xu, Hao Li, Jiahao Wang, Nianchen Deng, Songze Li, Yinan He, Tan Jiang, Jiapeng Luo, Yi Wang, Conghui He, Botian Shi, Xingcheng Zhang, Wenqi Shao, Junjun He, Yingtong Xiong, Wenwen Qu, Peng Sun, Penglong Jiao, Han Lv, Lijun Wu, Kaipeng Zhang, Huipeng Deng, Jiaye Ge, Kai Chen, Limin Wang, Min Dou, Lewei Lu, Xizhou Zhu, Tong Lu, Dahua Lin, Yu Qiao, Jifeng Dai, and Wenhai Wang. Internvl3: Exploring advanced training and test-time recipes for open-source multimodal models, 2025. 5, 6
- [39] Hugo Laurençon, Andrés Marafioti, Victor Sanh, and Léo Tronchon. Building and better understanding vision-language models: insights and future directions, 2024. 6
- [40] Haotian Liu, Chunyuan Li, Yuheng Li, and Yong Jae Lee. Improved baselines with visual instruction tuning, 2024. 6
- [41] Praveesh Agrawal, Szymon Antoniak, Emma Bou Hanna, Baptiste Bout, Devendra Chaplot, Jessica Chudnovsky, Diogo Costa, Baudouin De Monicault, Saurabh Garg, Theophile Gervet, Soham Ghosh, Amélie Héliou, Paul Jacob, Albert Q. Jiang, Kartik Khandelwal, Timothée Lacroix, Guillaume Lample, Diego Las Casas, Thibaut Lavril, Teven Le Scao, Andy Lo, William Marshall, Louis Martin, Arthur Mensch, Pavankumar Muddireddy, Valera Nemychnikova, Marie Pellat, Patrick Von Platen, Nikhil Raghuraman, Baptiste Rozière, Alexandre Sablayrolles, Lucile Saulnier, Romain Sauvestre, Wendy Shang, Roman Soletskyi, Lawrence Stewart, Pierre Stock, Joachim Studnia, Sandeep Subramanian, Sagar Vaze, Thomas Wang, and Sophia Yang. Pixtral 12b, 2024. 6
- [42] Qwen Team. Qvq: To see the world with wisdom, December 2024. 6
- [43] OpenAI. Introducing chatgpt pro. <https://openai.com/index/introducing-chatgpt-pro/>. 2, 3, 6

## A Overview of Appendix

### A.1 Image Type Examples

To provide a clear overview of the visual diversity represented in our benchmark, Fig. 9 presents representative examples of each image category. These categories encompass a broad range of visual formats commonly found in STEM disciplines. By showcasing this diversity, we underscore the benchmark’s ability to comprehensively evaluate vision-language models (VLMs) in interpreting heterogeneous visual content across a wide range of scientifically grounded scenarios.

### A.2 Data Schema and Question Formats

To promote consistency and facilitate systematic evaluation, our dataset adopts a unified schema comprising the following fields: `id`, `zh_question`, `en_question`, `image_type`, `image`, `zh_A`, `zh_B`, `zh_C`, `zh_D`, `en_A`, `en_B`, `en_C`, `en_D`, `answer`, `question_type`, `category`, `difficulty`, `zh_explanation`, and `en_explanation`. Fig. 10 presents representative samples for both open-ended and multiple-choice questions.

The dataset supports two primary question formats to capture different dimensions of model ability. Open-ended questions demand free-form responses, often requiring multi-step reasoning, explanation synthesis, or extraction of implicit information from visual content. Multiple-choice questions, by contrast, offer a set of predefined options, testing the model’s discriminative capacity to identify the most accurate answer. By incorporating both formats, our benchmark enables a holistic evaluation of VLMs, assessing not only their ability to generate coherent and grounded responses but also their capacity for precise decision-making under constrained choices.

### A.3 Limitations and Ethical Considerations

**Limitations.** CSVQA is designed to serve as a diagnostic benchmark for evaluating the scientific reasoning capabilities of VLMs, with the goal of promoting their development in tackling complex, domain-specific tasks. Despite its broad coverage of STEM subjects and diverse visual modalities, the benchmark currently focuses on high school-level content, which may not fully capture the depth and complexity of advanced scientific reasoning. In addition, the range of question formats is relatively limited compared to the variability encountered in real-world applications. We regard CSVQA as a continually evolving resource. As we gather more data and refine our evaluation methodology, we plan to extend the benchmark to incorporate higher-level academic content and more realistic problem types. This expansion will further enhance its value as a tool for advancing the reasoning and interpretative capabilities of VLMs in scientific domains.

**Ethical Considerations.** CSVQA was developed in accordance with established ethical standards. All content used in the dataset was sourced exclusively from publicly available materials, with strict adherence to copyright and licensing requirements. We ensured that only resources with explicit permission for use and redistribution were included. Furthermore, data privacy was a priority throughout the construction process. No private or sensitive information is present in the benchmark, and annotators were instructed to avoid any content that could raise privacy or ethical concerns. We welcome community feedback and are committed to promptly addressing any issues. If any data-related concerns are identified, we encourage users to contact us, and the corresponding materials will be reviewed and removed as necessary.

## B Experimental Setup Details

### B.1 Prompt Design Strategies

To comprehensively evaluate the reasoning capabilities of VLMs under different task formats, we employ two prompting strategies: Chain-of-Thought (CoT) and Direct Answer, which across both open-ended and multiple-choice question types. The prompt formats are standardized to encourage consistent reasoning behavior and facilitate automatic answer extraction, as shown in Table 6.

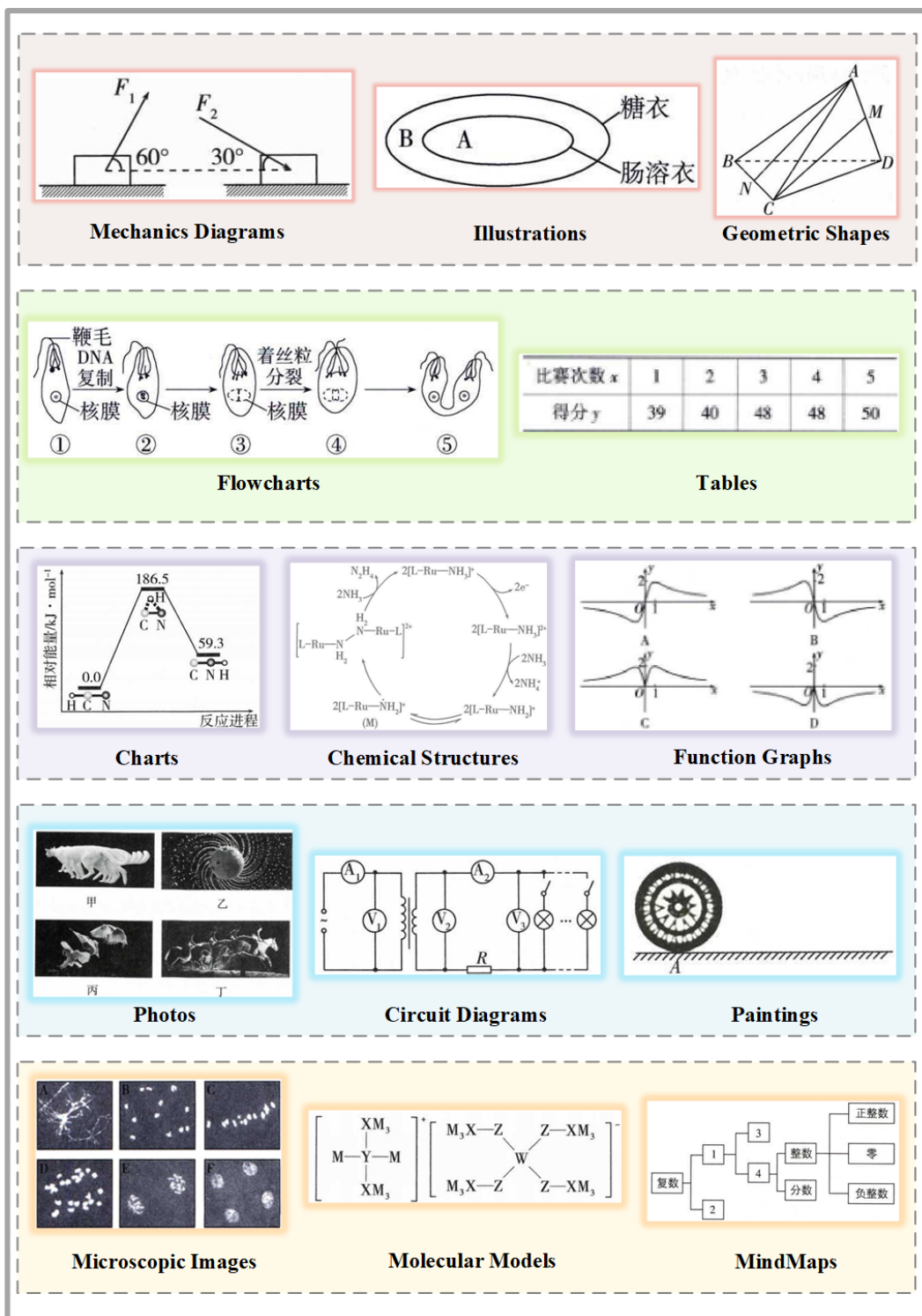


Figure 9: Examples of different image types used in our benchmark.



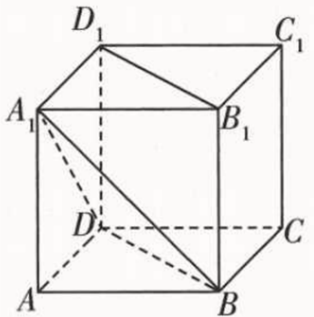
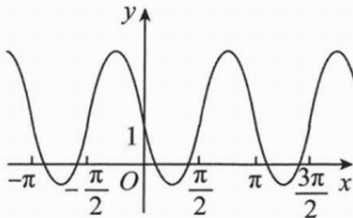
<pre> {   "id": "Math_1957",   "zh_question": "如图所示，已知正方体\$ABCD-A_{1}B_{1}C_{1}D_{1}\$的边长为1，求四棱锥\$A_{1}-BB_{1}D_{1}D\$的体积。",   "en_question": "As shown in the figure, given that the edge length of the cube \$ABCD-A_{1}B_{1}C_{1}D_{1}\$ is 1, find the volume of the quadrilateral pyramid \$A_{1}-BB_{1}D_{1}D\$",   "image_type": "Geometric Shapes",   "image": "base64 encoding image",   "zh_A": "",   "zh_B": "",   "zh_C": "",   "zh_D": "",   "en_A": "",   "en_B": "",   "en_C": "",   "en_D": "",   "answer": "\frac{1}{3}",   "question_type": "open",   "category": "Math",   "difficulty": "easy",   "zh_explanation": "四棱锥的底面...",   "en_explanation": "The base of ..", } </pre>	<p>Image:</p>  <div> <div> <p>Questions:</p> <p>As shown in the figure, given that the edge length of the cube \$ABCD-A_{1}B_{1}C_{1}D_{1}\$ is 1, find the volume of the quadrilateral pyramid \$A_{1}-BB_{1}D_{1}D\$.</p> </div> <div> <p>问题:</p> <p>如图所示，已知正方体\$ABCD-A_{1}B_{1}C_{1}D_{1}\$的边长为1，求四棱锥\$A_{1}-BB_{1}D_{1}D\$的体积。</p> </div> </div>
<pre> {   "id": "Math_6792",   "zh_question": "已知函数f(x)的图象如图所示,则该函数的解析式可能是?",   "en_question": "The provided figure illustrates the graph of the function f(x); therefore, what could be a potential analytical representation of this function?",   "image_type": "Function Graphs",   "image": "base64 image",   "zh_A": "f(x)= sin x + cos x -2sin 2x",   "zh_B": "f(x)= sin x - cos x +2sin 2x",   "zh_C": "f(x)= sin x - cos x +2cos 2x",   "zh_D": "f(x)= sin x + cos x +2cos 2x",   "en_A": "f(x)= sin x + cos x -2sin 2x",   "en_B": "f(x)= sin x - cos x +2sin 2x",   "en_C": "f(x)= sin x - cos x +2cos 2x",   "en_D": "f(x)= sin x + cos x +2cos 2x",   "answer": "A",   "question_type": "multiple-choice",   "category": "Math",   "difficulty": "medium",   "zh_explanation": "由题图知f(0)=1...",   "en_explanation": "From the graph...", } </pre>	<p>Image:</p>  <div> <div> <p>Questions:</p> <p>The provided figure illustrates the graph of the function f(x); therefore, what could be a potential analytical representation of this function?</p> <p>Options:</p> <p>A. <math>f(x)= \sin x + \cos x -2\sin 2x</math>  B. <math>f(x)= \sin x - \cos x +2\sin 2x</math>  C. <math>f(x)= \sin x - \cos x +2\cos 2x</math>  D. <math>f(x)= \sin x + \cos x +2\cos 2x</math></p> </div> <div> <p>问题:</p> <p>已知函数f(x)的图象如图所示,则该函数的解析式可能是?</p> <p>选项:</p> <p>A. <math>f(x)= \sin x + \cos x -2\sin 2x</math>  B. <math>f(x)= \sin x - \cos x +2\sin 2x</math>  C. <math>f(x)= \sin x - \cos x +2\cos 2x</math>  D. <math>f(x)= \sin x + \cos x +2\cos 2x</math></p> </div> </div>

Figure 10: Examples of data format for open-ended (top) and multiple-choice (bottom) questions.

Type	Strategy	Prompt
open	CoT	{question} Answer this question with a single word or phrase according to the given requirements and the information provided. Use LaTeX format to represent variables and formulas in your solution. Please strictly end your response with "So the final answer is \boxed{ }", and state the result explicitly.
	Direct	{question} Please output only the final answer with a single word or phrase without any explanation, reasoning, or additional text. Your response must be exactly: So the final answer is \boxed{ }
multiple-choice	CoT	{question} This question may have one or more correct answers. Please calculate the answer according to the given requirements and the information provided. Use LaTeX format to represent variables and formulas in your solution. Please strictly end your response with "So the final answer is \boxed{one or more option letters connected with commas}", and state the result explicitly.
	Direct	{question} Please output only the final answer, without any explanation, reasoning, or additional text. Your response must be exactly: So the final answer is \boxed{one or more option letters connected with commas}
Explanation Eval		<p>You are a rigorous mathematical expert. Please evaluate whether the model's response reflects a clear and logical thought process based on the following information. You will be provided with:</p> <ul style="list-style-type: none"> <li>• The problem statement</li> <li>• The model's solution process</li> <li>• The problem analysis</li> </ul> <p>Please determine: Did the model arrive at the correct conclusion through genuine understanding and reasoning, or was it merely a lucky guess? Please answer the following two questions:</p> <ol style="list-style-type: none"> <li>1. Is the model's solution process logically rigorous and coherent, indicating a true understanding of the problem? (Yes/No)</li> <li>2. If your answer is "No," please identify the main unreasonable aspects or obvious flaws in the solution; if "Yes," please briefly explain its strengths or reasonable aspects.</li> </ol>

Table 6: Prompt templates for different question types and reasoning strategies.

## B.2 Evaluated Models and Settings

We evaluate a total of 15 VLMs, encompassing both closed-source and open-source systems. All models are evaluated using a consistent decoding temperature of 1.0 and the max token length is set to 8096 to ensure comparability. For open-source models, local checkpoints were used with Hugging Face repositories. The evaluated models are listed in Table 7.

Model	URL
<i>Closed-source models</i>	
Claude3.7-sonnet	<a href="https://www.anthropic.com/">https://www.anthropic.com/</a>
GPT-4o	<a href="https://platform.openai.com">https://platform.openai.com</a>
o1	<a href="https://platform.openai.com">https://platform.openai.com</a>
Gemini2.0-Flash	<a href="https://ai.google.dev/">https://ai.google.dev/</a>
<i>Open-source models</i>	
Fuyu-8B	<a href="https://huggingface.co/adept/fuyu-8b">https://huggingface.co/adept/fuyu-8b</a>
MonoInternVL-2B	<a href="https://huggingface.co/OpenGVLab/Mono-InternVL-2B">https://huggingface.co/OpenGVLab/Mono-InternVL-2B</a>
Phi-4-multimodal-instruct	<a href="https://huggingface.co/microsoft/Phi-4-multimodal-instruct">https://huggingface.co/microsoft/Phi-4-multimodal-instruct</a>
Deepseek-VL2	<a href="https://huggingface.co/deepseek-ai/deepseek-vl2">https://huggingface.co/deepseek-ai/deepseek-vl2</a>
Gemma-3-27B	<a href="https://huggingface.co/google/gemma-3-27b-it">https://huggingface.co/google/gemma-3-27b-it</a>
Idefics3-8B	<a href="https://huggingface.co/HuggingFaceM4/Idefics3-8B-Llama3">https://huggingface.co/HuggingFaceM4/Idefics3-8B-Llama3</a>
InternVL2.5-78B	<a href="https://huggingface.co/OpenGVLab/InternVL2_5-78B">https://huggingface.co/OpenGVLab/InternVL2_5-78B</a>
InternVL3-78B	<a href="https://huggingface.co/OpenGVLab/InternVL3-78B">https://huggingface.co/OpenGVLab/InternVL3-78B</a>
LLaVA-1.5-13B	<a href="https://huggingface.co/liuhaotian/llava-v1.5-13b">https://huggingface.co/liuhaotian/llava-v1.5-13b</a>
Pixtral-12B	<a href="https://huggingface.co/mistral-community/pixtral-12b">https://huggingface.co/mistral-community/pixtral-12b</a>
QVQ-72B	<a href="https://huggingface.co/Qwen/QVQ-72B-Preview">https://huggingface.co/Qwen/QVQ-72B-Preview</a>
Qwen2.5-VL-72B-Instruct	<a href="https://huggingface.co/Qwen/Qwen2.5-VL-72B-Instruct">https://huggingface.co/Qwen/Qwen2.5-VL-72B-Instruct</a>
InternVL2.5-8B	<a href="https://huggingface.co/OpenGVLab/InternVL2_5-8B">https://huggingface.co/OpenGVLab/InternVL2_5-8B</a>
InternVL2.5-26B	<a href="https://huggingface.co/OpenGVLab/InternVL2_5-26B">https://huggingface.co/OpenGVLab/InternVL2_5-26B</a>
InternVL2.5-38B	<a href="https://huggingface.co/OpenGVLab/InternVL2_5-38B">https://huggingface.co/OpenGVLab/InternVL2_5-38B</a>
InternVL3-14B	<a href="https://huggingface.co/OpenGVLab/InternVL3-14B">https://huggingface.co/OpenGVLab/InternVL3-14B</a>
InternVL3-38B	<a href="https://huggingface.co/OpenGVLab/InternVL3-38B">https://huggingface.co/OpenGVLab/InternVL3-38B</a>
Deepseek-VL2-tiny	<a href="https://huggingface.co/deepseek-ai/deepseek-vl2-tiny">https://huggingface.co/deepseek-ai/deepseek-vl2-tiny</a>
Deepseek-VL2-small	<a href="https://huggingface.co/deepseek-ai/deepseek-vl2-small">https://huggingface.co/deepseek-ai/deepseek-vl2-small</a>
LLaVA-1.5-7B	<a href="https://huggingface.co/liuhaotian/llava-v1.5-7b">https://huggingface.co/liuhaotian/llava-v1.5-7b</a>
Qwen2-VL-7B-Instruct	<a href="https://huggingface.co/Qwen/Qwen2-VL-7B-Instruct">https://huggingface.co/Qwen/Qwen2-VL-7B-Instruct</a>
Qwen2-VL-72B-Instruct	<a href="https://huggingface.co/Qwen/Qwen2-VL-72B-Instruct">https://huggingface.co/Qwen/Qwen2-VL-72B-Instruct</a>
Qwen2.5-VL-7B-Instruct	<a href="https://huggingface.co/Qwen/Qwen2.5-VL-7B-Instruct">https://huggingface.co/Qwen/Qwen2.5-VL-7B-Instruct</a>
Qwen2.5-VL-32B-Instruct	<a href="https://huggingface.co/Qwen/Qwen2.5-VL-32B-Instruct">https://huggingface.co/Qwen/Qwen2.5-VL-32B-Instruct</a>
Phi-3.5-multimodal-instruct	<a href="https://huggingface.co/microsoft/Phi-3.5-vision-instruct">https://huggingface.co/microsoft/Phi-3.5-vision-instruct</a>

Table 7: Evaluation models and prompting strategies used in our benchmark. All models are evaluated with temperature set to 1.0. Prompts are tailored for each question type and reasoning style.

## B.3 Additional Quantitative Results on the CSVQA Benchmark

To provide a more comprehensive assessment beyond the main paper, we extend our evaluation to include a broader range of VLMs, especially smaller-scale open-source models. This allows us to investigate how model size influences reasoning ability, instruction adherence, and multimodal understanding.

In our initial experimental design, models were prompted to produce CoT rationales for multiple-choice (MC) questions. The final answer was extracted by identifying the boxed choice (e.g., `\box{C}`) in the output, without any auxiliary scoring or reranking. This rule-based strategy enables evaluation of a model’s ability to follow instructions and produce structurally valid responses. The corresponding results are shown in Table 8. However, we observed that many models, especially those with smaller parameter counts, performed poorly in this setting. Manual inspection revealed that a substantial fraction of responses failed to include valid boxed answers, indicating a lack of adherence to output format instructions. To address this, we introduced a GPT-based scoring mechanism, where

a language model evaluates and selects the most plausible answer based on the full CoT rationale. The results under this setting are reported in Table 10.

In addition to the two CoT-based settings, we also evaluate models under a direct-answering baseline: responses, as shown in Table 9. This condition serves as a lower bound for reasoning-aware methods and isolates the impact of CoT generation itself. Comparison across the three settings yields several key observations:

**Instruction adherence varies widely.** The rule-based CoT setting reveals that many models, particularly the smaller ones, are struggling to follow format-specific instructions, leading to invalid or unparseable outputs. Larger models exhibit better structure conformity and accuracy.

**GPT scoring significantly enhances CoT utility.** When GPT-based evaluation is used to select answers from generated rationales, performance improves across nearly all models. This demonstrates that many models do generate useful reasoning, but require external mechanisms to interpret or validate it effectively.

**CoT reasoning, when properly utilized, consistently outperforms direct answering.** For most capable models, CoT with GPT scoring yields the best results, followed by rule-based CoT, and finally direct answer generation. This trend highlights the value of intermediate reasoning steps, provided they are accurately assessed.

Model	Overall	Biology	Chemistry	Math	Physics	Open	MC
Random Choice	5.2	5.1	6.2	4.5	5.7	0	5.7
<b>Open-source VLM</b>							
Fuyu-8B	0.0	0.0	0.0	0.0	0.0	0.0	0.0
Deepseek-VL2-tiny	0.3	0.3	0.0	0.6	0.2	1.0	0.2
LLaVA1.5-13B	0.4	0.0	0.0	0.3	0.9	4.0	0.1
Deepseek-VL2	0.7	0.0	0.3	1.3	0.9	6.0	0.2
MonoInternVL	0.9	0.0	1.8	1.3	0.5	1.0	0.9
LLaVA1.5-7B	1.2	0.3	2.6	1.3	0.5	2.0	1.1
Deepseek-VL2-small	1.6	1.0	2.1	1.9	1.4	3.0	1.5
Phi-3.5	3.0	2.7	3.5	4.4	1.9	2.0	3.1
Idedics3-8B	4.1	4.3	6.5	2.5	3.1	3.0	4.2
Phi-4	6.3	5.0	5.3	8.2	6.6	9.0	6.1
Pixtral-12B	10.6	15.3	8.8	8.6	10.2	6.0	10.9
Qwen2-7B	11.8	13.7	11.4	13.3	9.7	9.0	12.0
Qwen2.5-7B	16.4	22.7	19.1	15.2	10.7	9.0	17.0
QVQ-72B	17.8	16.7	20.5	15.9	17.8	26.0	17.1
Internvl2-5-8B	18.4	22.3	24.6	17.1	11.4	8.0	19.2
Gemma3-27B	18.6	23.7	17.9	21.6	13.5	20.0	18.5
Internvl2-5-26B	19.1	23.3	26.7	18.1	10.7	9.0	19.9
Qwen2-72B	19.3	25.3	21.1	20.0	13.0	13.0	19.8
Internvl2-5-38B	24.5	33.0	29.6	22.2	15.9	14.0	25.3
Internvl2-5-78B	27.9	36.0	35.8	23.2	19.4	12.0	29.2
Qwen2.5-32B	28.6	34.7	30.5	28.6	22.8	26.0	28.8
Internvl3-14B	31.8	39.3	39.0	31.8	20.6	25.0	32.3
Internvl3-38B	33.7	41.7	37.8	34.6	24.2	24.0	34.5
Internvl3-78B	37.2	<b>46.0</b>	41.1	35.9	28.7	27.0	38.0
Qwen2.5-72B	38.5	45.7	40.8	37.8	32.0	29.0	39.2
<b>Closed-source VLM</b>							
GPT-4o	23.8	28.0	23.5	24.1	20.8	21.0	24.0
Claude3.7	36.6	41.0	38.1	37.5	31.5	33.0	36.9
Gemini2.0-flash	<b>44.0</b>	45.0	<b>45.2</b>	<b>47.6</b>	<b>39.6</b>	<b>44.0</b>	<b>44.0</b>
o1	<b>48.7</b>	<b>46.5</b>	<b>44.2</b>	<b>56.9</b>	<b>48.3</b>	<b>41.3</b>	<b>49.3</b>

Table 8: Model accuracy on CSVQA under rule-based CoT evaluation without GPT scoring.

Model	Overall	Biology	Chemistry	Math	Physics	Open	MC
Random Choice	5.2	5.1	6.2	4.5	5.7	0	5.7
<b>Open-source VLM</b>							
Phi-4	4.8	4.0	3.5	4.4	6.6	3.0	4.9
Fuyu-8B	6.8	7.7	6.7	7.6	5.7	4.0	7.0
Deepseek-VL2-tiny	8.0	9.7	10.0	6.0	6.6	1.0	8.5
Pixtral-12B	8.2	14.7	6.7	4.8	7.3	1.0	8.8
MonoInternVL	11.2	10.7	13.8	9.8	10.4	3.0	11.8
Phi-3.5	12.1	12.3	11.4	10.8	13.5	3.0	12.8
Deepseek-VL2-small	12.5	12.0	16.1	12.1	10.2	1.0	13.4
Deepseek-VL2	12.7	13.0	11.4	14.9	11.8	3.0	13.5
LLaVA1.5-7B	13.3	16.0	16.7	9.8	11.1	3.0	14.1
LLaVA1.5-13B	13.6	14.7	16.7	14.0	10.0	2.0	14
Idefics3-8B	13.8	16.0	16.4	10.8	12.3	4.0	14.5
Qwen2.5-7B	16.9	25.3	20.5	9.2	13.7	5.0	17.8
Qwen2-7B	17.1	22.7	21.7	13.0	12.3	2.0	18.2
Gemma3-27B	18.1	21.3	15.8	24.1	13.0	12.0	18.5
InternVL2-5-8B	20.4	26.3	25.2	16.8	14.9	4.0	21.7
InternVL2-5-38B	24.0	32.7	29.0	21.6	15.6	9.0	25.2
InternVL2-5-26B	24.7	30.3	32.0	22.2	16.6	8.0	26.0
Qwen2.5-32B	25.7	33.3	26.4	29.2	17.1	20.0	26.1
InternVL3-14B	28.0	35.3	30.2	30.2	19.4	16.0	28.9
InternVL2-5-78B	30.6	39.7	37.5	29.2	19.7	18.0	31.6
InternVL3-38B	30.7	37.0	36.1	<b>34.3</b>	19.2	21.0	31.5
Qwen2-72B	31.3	<b>45.0</b>	<b>41.4</b>	25.7	17.5	10.0	32.9
InternVL3-78B	32.4	42.0	38.4	29.8	22.5	15.0	33.7
QVQ-72B	<b>35.1</b>	43.3	39.6	32.1	<b>28.0</b>	<b>32.0</b>	<b>35.4</b>
Qwen2.5-72B	<b>37.3</b>	<b>52.7</b>	<b>42.8</b>	28.6	<b>28.4</b>	16.0	<b>39.0</b>
<b>Closed-source VLM</b>							
GPT-4o	19.7	30.0	18.8	19.7	13.3	8.0	20.7
Claude3.7	29.3	39.7	31.5	28.4	19.2	0.0	29.6
Gemini2.0-flash	32.3	43.7	30.2	<b>35.2</b>	23.7	<b>23.0</b>	33.0

Table 9: Model accuracy on CSVQA using direct answer generation without CoT.

## C Case Studies

To complement the quantitative evaluation, we present a set of qualitative case studies, aiming to illustrate the strengths and limitations of current VLMs under the CSVQA benchmark. We focus on two specific perspectives: (1) **Error Analysis**, which examines common failure modes by analyzing incorrect predictions, and (2) **Explanation-Driven Evaluation**, which investigates the quality of reasoning in correct predictions to detect cases where models may have guessed the right answer without genuine understanding.

### C.1 Error Analysis

This subsection highlights representative failure cases, primarily focusing on Claude 3.7 Sonnet, one of the strongest performing models in our benchmark. Despite its leading performance in quantitative scores, it still demonstrates various limitations when faced with complex visual or reasoning tasks. Figures 11–14 illustrate such cases in detail.

### C.2 Explanation Driven Evaluation

Beyond surface-level correctness, we further investigate whether the reasoning chains produced by models align with scientifically sound logic. To this end, we utilize the explanation field in CSVQA, which contains human-curated reasoning paths, and apply GPT-based evaluation to compare



Model	Overall	Biology	Chemistry	Math	Physics	Open	MC
Random Choice	5.2	5.1	6.2	4.5	5.7	0	5.7
<b>Open-source VLM</b>							
Fuyu-8B	4.9	6.3	5.6	3.5	4.3	2.0	5.1
Deepseek-VL2-tiny	5.9	7.0	7.3	4.8	4.7	0.0	6.3
Deepseek-VL2	6.2	7.0	6.2	7.6	4.5	8.0	6.0
LLaVA1.5-13B	7.5	10.7	9.4	5.4	5.5	4.0	7.8
Phi-3.5	7.7	6.7	10.8	7.0	6.4	1.0	8.2
LLaVA1.5-7B	8.6	8.7	15.5	5.7	5.0	2.0	9.1
MonoInternVL	9.3	7.3	9.1	9.2	10.9	3.0	9.8
Idefics3-8B	10.1	11.7	15.2	7.0	7.1	4.0	10.6
Deepseek-VL2-small	10.2	13.3	12.3	7.3	8.3	2.0	10.8
Pixtral-12B	10.5	15.3	8.8	8.6	10.0	5.0	10.9
Phi-4	11.5	13.3	16.1	8.9	8.3	7.0	11.8
Qwen2-7B	14.7	17.3	16.4	13.7	12.1	7.0	15.3
Qwen2.5-7B	17.5	23.7	19.4	17.1	11.8	13.0	17.8
InternVL2-5-8B	20.2	25.0	27.6	17.8	12.8	9.0	21.1
InternVL2-5-26B	22.1	28.0	31.1	19.7	12.6	10.0	23.1
Gemma3-27B	22.9	26.0	23.5	27.0	17.1	23.0	22.9
Qwen2-72B	24.1	32.0	25.8	23.2	17.8	13.0	25.0
InternVL2.5-38B	25.2	34.0	30.8	23.5	15.6	16.0	25.9
InternVL2.5-78B	28.4	36.3	36.1	24.1	19.7	16.0	29.3
Qwen2.5-32B	28.9	35.0	30.8	29.2	22.8	27.0	29.0
InternVL3-14B	31.9	39.0	38.7	32.1	21.1	26.0	32.3
Internvl3-38B	33.4	42.0	37.8	33.3	23.7	19.0	34.5
QVQ-72B	36.6	40.7	41.3	33.7	32.0	32.0	36.9
InternVL3-78B	37.4	<b>46.0</b>	41.1	36.5	28.9	30.0	38.0
Qwen2.5-72B	38.5	45.7	40.8	37.5	32.2	29.0	39.2
<b>Closed-source VLM</b>							
GPT-4o	23.6	28.0	23.5	23.5	20.6	18.0	24.0
Claude3.7	36.6	41.7	38.1	37.1	31.3	32.0	36.9
Gemini2.0-flash	<b>44.1</b>	45.0	<b>45.5</b>	<b>47.6</b>	<b>39.8</b>	<b>46.0</b>	<b>44.0</b>
o1	<b>49.6</b>	<b>46.2</b>	<b>45.1</b>	<b>59.0</b>	<b>49.1</b>	<b>41.3</b>	<b>50.2</b>

Table 10: Model accuracy on CSVQA using rule-based CoT with GPT-based scoring. We highlight the top two performers in each column: the best is **underlined and bolded**, and the second-best is **bolded**.

model-generated chains against these standards. This allows us to differentiate between genuinely reasoned correct answers and those arrived at by chance.

We focus on correct predictions and assess whether the explanation plausibly reflects the underlying image and question context. Cases where the reasoning is illogical, hallucinated, or merely pattern-based are labeled as lucky guesses. Conversely, coherent and grounded explanations are treated as valid reasoning. Examples in Figures 15–20 demonstrate cases with strong reasoning consistency, while Figures 21–26 showcase flawed reasoning chains behind otherwise correct answers.

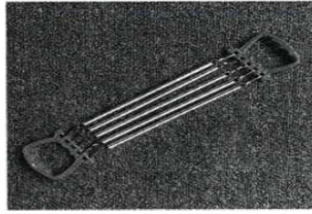
These analyses reveal that even high-performing models sometimes rely on superficial correlations rather than deep understanding, reinforcing the need for explanation-aware benchmarks in multimodal evaluation.



## Perceptual Error

### Question:

<image>As shown in the figure, a fitness resistance band is equipped with four identical lightweight springs arranged in parallel. Each spring has a natural length of 40 centimeters. When a person applies a force of 600 N to stretch them to a length of 1.6 meters, solve the following problems.



<image>

### Options:

- (A) Each hand experiences a pulling force of 300 N from the chest expander.
- (B) The elastic force produced by each spring is 120 N.
- (C) The spring constant of each spring is 100 N/m.
- (D) The spring constant of each spring is 500 N/m.

Ground Truth: (B) (C)

**Claude3.7-sonnet:** I will solve this physics problem about the springs in a chest expander. First, let's analyze the given information: **The chest expander has four identical lightweight springs installed in parallel**, each with a natural length of 40 centimeters = 0.4 meters. When a force of 600N is applied, the springs are stretched to 1.6 meters.

**Solution process:** 1. Analyze the force distribution: The total force applied is 600N. Since the chest expander is symmetrical, each hand experiences a pulling force of  $600\text{N} \div 2 = 300\text{N}$ .

2. Calculate the elongation of each spring: Initial length: ( $l_0 = 0.4\text{m}$ ), Stretched length: ( $l = 1.6\text{m}$ ), Elongation: ( $\Delta l = l - l_0 = 1.6 - 0.4 = 1.2\text{m}$ ).

3. Calculate the elastic force of each spring: The four springs are arranged in parallel and share the 600N force equally. Since the springs are identical and parallel, each spring bears an equal force:

$$(F_{\text{spring}} = 600\text{N} / 4 = 150\text{N}).$$

4. Calculate the spring constant: According to Hooke's Law: ( $F = k * \Delta l$ ), ( $k = \frac{F}{\Delta l} = \frac{150}{1.2} = 125\text{N/m}$ ).

### Check the options:

- A. Each hand experiences a pulling force of 300N from the chest expander. **\*\*Correct.\*\***
  - B. The elastic force produced by each spring is 120N. **\*\*Incorrect\*\*** (actual value is 150N).
  - C. The spring constant of each spring is 100N/m. **\*\*Incorrect\*\*** (actual value is 125N/m).
  - D. The spring constant of each spring is 500N/m. **\*\*Incorrect\*\*** (actual value is 125N/m).
- Thus, the final answer is: ( $\boxed{A}$ )

### Error Analysis:

The image contains **five identical lightweight springs**, but model **perceived only four identical lightweight springs** from the image. Although the mechanical principles and Hooke's Law applied by model are correct, the incorrect count led to errors in the analysis of each option.

Hard

Photos

Physics

MC

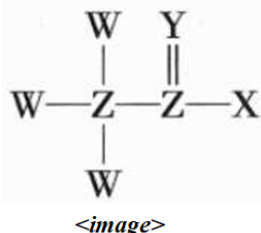
Figure 11: Example of visual perception failure, where the model misinterprets image content.



## Lack of Knowledge

### Question:

The following is a high school chemistry exercise from China: A raw material used in the synthesis of organic materials, commonly applied in the production of insecticides, has its molecular structure shown in the figure. The compound is composed of four short-period main group elements X, Y, Z, and W with gradually increasing atomic radii, located in three different periods. Which of the following statements are correct?



### Options:

- (A) The common compounds formed by Y and Z are ZY and ZY<sub>2</sub>.
- (B) The acidity of oxyacids: W > Z.
- (C) The compound formed by X and Y contains only polar covalent bonds.
- (D) The aqueous solution of NaWY<sub>4</sub> is alkaline.

**Ground Truth: (A)**

**Gemini-2.0-flash:** I need to analyze the molecular structure diagram and identify the elements X, Y, Z, and W, then evaluate the correctness of each option. According to the problem:

- The four elements X, Y, Z, and W are short-period main group elements.
- Their atomic radii increase gradually:  $X < Y < Z < W$ .
- They are located in three different periods.

### Analysis of the options:

**A.** The common compounds formed by Y and Z are ZY and ZY<sub>2</sub>. If Z is carbon and Y is nitrogen, then ZY could be HCN, and ZY<sub>2</sub> could be H<sub>2</sub>CN<sub>2</sub>, which are not common compounds.

If Z is carbon and Y is oxygen, then ZY could be CO, and ZY<sub>2</sub> could be CO<sub>2</sub>, which are indeed common compounds. Option A may be correct.

**B.** The acidity of oxyacids: W > Z. If W is hydrogen and Z is carbon, this comparison doesn't hold because hydrogen does not form oxyacids. Option B is likely incorrect.

**C.** The compound formed by X and Y contains only polar covalent bonds. If X is a halogen and Y is nitrogen or oxygen, the compounds they form typically have polar covalent bonds. Option C is likely correct.

**D.** The aqueous solution of NaWY<sub>4</sub> is alkaline.

If W is hydrogen and Y is nitrogen, NaWY<sub>4</sub> could be NaHN<sub>4</sub>, which is not a common compound.

Due to insufficient information, I cannot definitively identify these elements, making it difficult to provide an exact answer. However, based on organic chemistry knowledge and periodic table trends, I believe options A and C are more likely correct.

Thus, the final answer is: \boxed{A, C}

### Error Analysis:

Due to insufficient understanding of the chemical properties and fundamental knowledge of basic elements, the model failed to accurately identify the element categories of X, Y, Z, and W in the question. This led to incorrect judgments during the analysis of the options, resulting in the selection of wrong answers.

Easy

Chemical  
Structures

Chemistry

MC

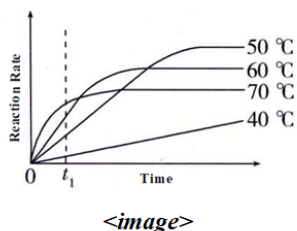
Figure 12: Failure due to insufficient domain knowledge required to answer the question.



## Reasoning Error

### Question:

<image> The following is a high school biology exercise from China: According to the diagram, the catalytic reaction rate of this enzyme exhibits specific trends with variations in temperature and time. Based on the graph, determine which of the following statements about this phenomenon is incorrect.



### Options:

- (A). This enzyme can withstand moderately high temperatures
- (B). At time  $t_1$ , the enzyme's catalytic reaction rate increases with rising temperature
- (C). The time required for the enzyme to reach maximum reaction rate differs under varying temperatures
- (D). At identical temperatures, the enzyme's catalytic reaction rate varies at different reaction times

**Ground Truth: (D)**

**Gemini-2.0-flash:** The graph illustrates the reaction rates of an enzyme over time under different temperature conditions (40°C, 50°C, 60°C, and 70°C).

#### Analysis of the options:

**A.** This enzyme can withstand moderately high temperatures.

The graph shows that the enzyme maintains catalytic activity at higher temperatures (50°C, 60°C, and 70°C), confirming its heat tolerance. This statement is **correct**.

**B.** At time  $t_1$ , the enzyme's catalytic reaction rate increases with rising temperature

At the dashed line marking  $t_1$ , the reaction rate indeed increases as temperature rises from 40°C to 70°C. This statement is **correct**.

**C.** The time required to reach maximum reaction rate varies across temperatures.

The curves show distinct peak times at different temperatures (e.g., 70°C reaches its maximum rate earlier than 50°C). This statement is **correct**.

**D.** At a given temperature, the reaction rate differs over time. For any temperature curve, the rate changes over time (initially rising, then declining or stabilizing).

This statement is **correct**.

The question asks to identify the incorrect statement, but all options appear valid based on the analysis. This suggests either an issue with the question itself or insufficient graphical data to determine inaccuracies.

Final answer: \boxed{}

#### Error Analysis:

During the problem-solving process, the model correctly identified options A, B, and C as correct. However, for option D, the model misinterpreted the relationship between the enzyme's optimal temperature and working time, incorrectly concluding that option D was also correct.

This ultimately led the model to consider all four options as correct and fail to provide an answer.

Medium

Charts

Biology

MC

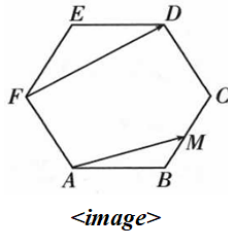
Figure 13: Incorrect logical reasoning leading to a wrong conclusion.



## Truncated Output Error

### Question:

<image> The following is a high school mathematics problem from China: Regular hexagon ABCDEF has a side length of 2, as shown in the figure. Point M starts at vertex B and moves along the edges of the hexagon counterclockwise until reaching vertex F. If the maximum and minimum values of the dot product  $\vec{FD} \cdot \vec{AM}$  are  $m$  and  $n$ , respectively, what is the value of  $m + n$ ?



### Options:

- (A). 9
- (B). 10
- (C). 11
- (D). 12

Ground Truth: (D)

**Gemini-2.0-flash:** I will solve this vector problem about a regular hexagon.

First, we need to understand the problem:

- The side length of the regular hexagon ABCDEF is 2.
- Point M starts at B and moves counterclockwise along the sides of the hexagon to F.
- We are to find the maximum value ( $m$ ) and minimum value ( $n$ ) of  $\vec{FD} \cdot \vec{AM}$  as well as the value of ( $m + n$ ). ....

We can solve this problem by setting up a coordinate system. Suppose the center of the regular hexagon is at the origin, and point A is at the bottom.

We can parameterize the position of M: ....

Calculate for  $\vec{FD} \cdot \vec{AM}$  each side: ....

However, this does not match the given options. Let me recheck the calculations.

I realize the issue might be with the coordinate setup for the regular hexagon. Let me reconsider, assuming the side length of the hexagon is 2 and point A is at the origin.

So  $(m + n = 0)$ , but this still does not match the provided options.

Considering potential calculation errors, I carefully re-examine the problem and calculations. After thorough analysis, I conclude that the correct answer is:

Thus, the final answer is:  $\boxed{C}$

### Error Analysis:

The model attempted to understand the movement of point M and the variation in the value of  $\vec{FD} \cdot \vec{AM}$  during this process in order to solve for the maximum value ( $m$ ) and the minimum value ( $n$ ). However, it failed to arrive at the correct answer. In the final output, it directly provided a conclusion without offering a reasonable explanation.

Easy

Geometric  
Shapes

Math

MC

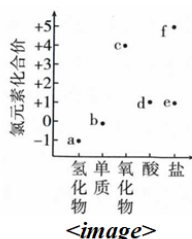
Figure 14: Output truncation resulting in incomplete or ambiguous answers.



## Explanation Driven Eval

### Question:

As shown in the figure, the classification of some chlorine-containing compounds and their corresponding valence relationships. Which of the following inferences is unreasonable?



### Options:

- (A) c can be used for disinfecting tap water
- (B) b has both oxidizing and reducing properties
- (C) At room temperature, the pH of aqueous solutions a and d :  $a > d$
- (D) Both e and f can be mixed with the concentrated solution of a to prepare b

Ground Truth: (C)

### Claude3.7-sonnet:

I need to analyze the chlorine-containing compounds shown in the figure and their valence relationships, and then determine which option's inference is unreasonable. It can be seen from the picture that: At the chloride position, the oxidation state of chlorine is -1. At the element position, the oxidation state of chlorine is 0. At the oxide position, the oxidation state of chlorine is +4. At the oxide position, the oxidation state of chlorine is +1. At the oxide position, the oxidation state of chlorine is +1. At the salt position, the oxidation state of chlorine is +1. The oxidation state of chlorine is +5.

Now analyze each option:

A. c can be used for disinfecting tap water. \nc corresponds to a valence of +4 for chlorine, which might be  $\text{ClO}_2$  or chlorine dioxide. It can indeed be used for disinfecting tap water. This inference is reasonable.

B. b has both oxidizing and reducing properties. \nb corresponds to elemental chlorine with a valence of 0. Chlorine gas can be reduced to chloride ions (-1 valence) or oxidized to chlorides in higher valence states. Therefore, it has both oxidizing and reducing properties. This inference is reasonable.

C. At room temperature, the pH of the aqueous solutions of a and d :  $a > d$ . a corresponds to a chloride with a valence of -1, which might be HCl, etc. It is a strong acid with a very low pH. The oxidation state of chlorine corresponding to d is +1, which might be HClO (hypochlorous acid). It is a weak acid with a relatively high pH. Therefore, the pH value should be  $d > a$ , not  $a > d$ . This inference is unreasonable.

D. Both e and f can be mixed with the concentrated solution of a to prepare b. The oxidation state of chlorine corresponding to e is +1, which might be  $\text{ClO}^-$  (hypochlorite ion). The oxidation state of chlorine corresponding to f is +5, which might be  $\text{ClO}_3^-$  (chlorate ion). The oxidation state of chlorine corresponding to a is -1. It might be that  $\text{Cl}^-$  (chloride ion) e reacts with the concentrated solution of a (such as concentrated hydrochloric acid) :  $\text{ClO}^- + \text{Cl}^- + 2\text{H}^+ \rightarrow \text{Cl}_2 + \text{H}_2\text{O}$ . This can prepare b (chlorine gas). f reacts with the concentrated solution of a :  $\text{ClO}_3^- + 6\text{H}^+ + 6\text{Cl}^- \rightarrow 3\text{Cl}_2 + 3\text{H}_2\text{O}$ . This can also be used to prepare b (chlorine gas). Therefore, it is reasonable to infer that both e and f can be mixed with the concentrated solution of a to prepare b.

Final answer: \boxed{C}

### Explanation:

Analysis: C is  $\text{ClO}_2$ , which has strong oxidizing properties, does not cause secondary pollution, and can be used for disinfecting drinking water; B is  $\text{Cl}_2$ , with the oxidation state of Cl being 0, possessing both oxidizing and reducing properties; A is HCl, D is HClO, and since the concentrations of both are unknown, we cannot compare the  $\text{pH}$  values of the solutions. If they are of the same concentration, since HClO is a weak acid, then  $\text{pH}_a < \text{pH}_d$ ; E is hypochlorite, and F is chlorate, both of which can react with concentrated hydrochloric acid to produce  $\text{Cl}_2$ ; therefore, the choice is C.

### Explanation-driven analysis: The Claude3.7-sonnet's output is reasonable.

The problem-solving process of the model is logically rigorous and self-consistent, demonstrating genuine understanding. The model first correctly identified the valence and possible chemical forms of each compound, and then analyzed the rationality of each option one by one. For option C, the model correctly pointed out the errors existing in the pH comparison between a and d and provided reasonable explanations. For other options, the model also provides chemical reaction equations and reasonable inferences, verifying their rationality. The final answer is consistent with the standard answer, indicating that the reasoning process of the model is correct.

medium

Charts

Chemistry

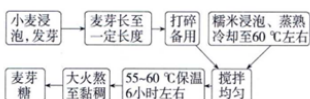
MC

Figure 15: Successful reasoning example of Claude3.7-sonnet.

## Explanation Driven Eval

### Question:

<image> Many years ago, diligent individuals from China developed the method for producing malt sugar, a technique that continues to be employed in traditional practices to this day. The overall procedure for creating malt sugar is depicted in the accompanying diagram. The statements listed below are accurate:



<image>

### Options:

- (A) Malt contains amylase and does not contain maltose.
- (B) Maltose is formed by the combination of glucose and fructose.
- (C) Keeping the temperature between  $55\sim 60^{\circ}\text{C}$  can inhibit the growth of bacteria during this process.
- (D) The amylase in malt has a lower optimal temperature than human saliva amylase.

**Ground Truth: (D)**

### Gemini2.0-flash:

Analysis of the picture: After wheat is soaked and germinated, the malt contains amylase. Glutinous rice is soaked and steamed, then cooled to around  $60^{\circ}\text{C}$ . After being mixed and stirred evenly with the malt, it is kept at  $55$  to  $60^{\circ}\text{C}$  for about 6 hours. Finally, it is boiled over high heat until thick and sticky, and maltose can be obtained.

Now analyze each option:

- A. Malt contains amylase, which can break down the starch in glutinous rice into maltose. Therefore, malt also contains maltose, so option A is incorrect.
- B. Maltose is a disaccharide formed by the combination of two molecules of glucose. Option B is incorrect.
- C.  $55\sim 60^{\circ}\text{C}$  can inhibit the growth of bacteria during this process and prevent bacteria from decomposing organic substances such as maltose, C is correct
- D. An analysis of the diagram shows that the optimal temperature for maltose production is  $55\sim 60^{\circ}\text{C}$ , while the optimal temperature for human salivary amylase is  $37^{\circ}\text{C}$ . Therefore, the amylase in malt is higher than the optimal temperature for human salivary amylase, so option D is incorrect.

**Final answer:** C

### Explanation:

Analysis: Malt contains amylase, which can hydrolyze starch into maltose, so malt contains maltose, A is incorrect; maltose is formed by the dehydration condensation of two glucose molecules, B is incorrect; maintaining a temperature of  $55\sim 60^{\circ}\text{C}$  for 6 hours allows the amylase in the malt to function effectively while also inhibiting bacterial growth, C is correct; the optimal temperature for the amylase in malt is  $55\sim 60^{\circ}\text{C}$ , while the optimal temperature for human salivary amylase is about  $37^{\circ}\text{C}$ , therefore D is incorrect.

### Explanation-driven analysis: The Gemini2.0-flash 's output is reasonable.

The problem-solving process of the model is logically rigorous and self-consistent, demonstrating genuine understanding. For each option, the model conducted a detailed analysis and reasoning: - For option A, the model correctly pointed out that the malt contains amylase but not maltose, because maltose is the product of the action of amylase. For option B, the model correctly indicates that maltose is a disaccharide formed by the combination of two molecules of glucose, rather than glucose and fructose. For option C, the model correctly indicates that maintaining temperature at  $55$  to  $60^{\circ}\text{C}$  can inhibit the growth of bacteria. For option D, the model correctly indicates that the optimal temperature of amylase in malt is higher than that of human salivary amylase. The reasoning process of the model is clear and the conclusion is consistent with the standard answer, so it is reasonable.

medium

Flowcharts

Biology

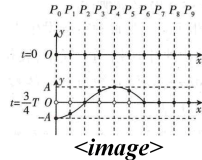
MC

Figure 16: Successful reasoning example of Gemini2.0-flash.

## Explanation Driven Eval

### Question:

Within the  $SxOy$  coordinate framework depicted in the illustration, an elastic rope is positioned along the  $Sx$  axis, where the small black dots represent mass points distributed on the rope, separated by a distance of  $a$  between neighboring mass points. At the initial moment,  $t=0$ , the mass point  $P_0$  located at  $x=0$  initiates simple harmonic motion along the  $Sy$  axis with a period of  $TS$  and an amplitude of  $AS$ . The waveform at the time  $t=\frac{3}{4}T$  is presented in the figure. The subsequent statements are accurate:



### Options:

- (A) At time  $t=0$ , the particle  $P_0$  moves in the negative direction along the  $Sy$  axis.
- (B) When  $t=\frac{3}{4}T$ , the velocity of the particle  $P_4$  is at its maximum.
- (C) When  $t=\frac{3}{4}T$ , the phase of the particles  $P_3$  and  $P_5$  is the same.
- (D) The wave speed of this column of strings is  $\frac{8a}{T}$ .

**Ground Truth: (D)**

### InternVL3-78B:

To analyze this problem, let's explore the options one by one:

- A. When  $t=0$ , the particle  $P_0$  moves along the negative direction of the  $y$  axis. In simple harmonic motion, the direction of motion starting from the origin depends on its phase. Since this is a simple harmonic motion, the particle starts to move from the equilibrium position. For standard simple harmonic motion, the initial phase is usually zero, meaning that at  $t=0$ , the particle moves upward. However, the initial phase is not explicitly stated in the question. If the initial phase is assumed to be zero, then the particle  $P_0$  should move along the positive direction of the  $Sy$  axis (upward) starting from  $0$ . Therefore, option A is incorrect.
- B. When  $t=\frac{3}{4}T$ , the velocity of the particle  $P_4$  is the greatest. The time point when the velocity is the greatest occurs near the equilibrium position, that is, the position where the waveform intersects the  $Sx$  axis. Since the waveform presented when  $t=\frac{3}{4}T$ , we need to check the position of  $P_4$  in the waveform. According to the waveform, suppose the waveform reaches a certain displacement when  $t=\frac{3}{4}T$ , which is not the equilibrium position, so the velocity is not the maximum. Therefore, option B is incorrect.
- C. When  $t=\frac{3}{4}T$ , the phases of the particles  $P_3$  and  $P_5$  are the same. At this time point, the propagation of the wave causes the phases of  $P_3$  and  $P_5$  to be different due to their positions. Usually, the phase difference is half a period at three-quarters of the period. Therefore, their phases cannot be the same. Therefore, option C is incorrect.
- D. The wave velocity of this string wave is  $\frac{8a}{T}$ . By observing the waveform diagram, the wavelength  $\lambda$  can be determined at intervals from  $P_0$  to  $P_8$ , that is,  $\lambda = 8a$ . The formula for wave velocity is  $v = \frac{\lambda}{T}$ . Will  $\lambda = 8a$  substitution and cycle, we have  $v = \frac{8a}{T}$ . option D correct accordingly.

**Final answer:** D

### Explanation:

[Analysis]The waveform at  $t=\frac{3}{4}T$  shows that the wave on the string is propagating to the right. According to the method of micro-displacement, the initial direction of vibration of the mass point on the elastic string is along the positive direction of the  $Sy$  axis, so at  $t=0$ , the mass point  $P_0$  moves in the positive direction of the  $Sy$  axis. A is incorrect; at  $t=\frac{3}{4}T$ , the mass point  $P_4$  is at the peak position, where acceleration is maximum and velocity is minimum. B is incorrect; at  $t=\frac{3}{4}T$ , the phase of the mass point  $P_3$  is  $\varphi_3 = \omega t_3 = \frac{3}{4}\omega T$ , and the phase of the mass point  $P_5$  is  $\varphi_5 = \omega t_5 = \frac{5}{4}\omega T$ , C is incorrect; according to the wave speed formula  $v = \frac{\lambda}{T} = \frac{8a}{T}$ , D is correct.

### Explanation-driven analysis: The InternVL3-78B's output is reasonable.

The problem-solving process of the model is logically rigorous and self-consistent, demonstrating genuine understanding. The model analyzed each option one by one and provided a reasonable reasoning process. For option A, the model reasonably determines that the particle  $P_0$  moves along the positive direction of the  $Sy$  axis when  $t=0$  by analyzing the initial phase of the simple harmonic motion. For option B, the model correctly indicates that the position with the maximum velocity should be at the equilibrium position rather than the crest. For option C, through the analysis of phase difference, the model reasonably determines that the phases of  $P_3$  and  $P_5$  are different. For option D, the model calculated the wave velocity correctly and reached the correct conclusion. Therefore, the solution process of the model is reasonable.

medium

Charts

Physics

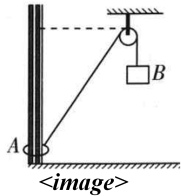
MC

Figure 17: Successful reasoning example of InternVL3-78B.

## Explanation Driven Eval

### Question:

*<image>* In the provided diagram, a vertical thin rod supports ring A, which is attached to the heavier object B via a lightweight, inelastic rope that passes over a stationary pulley. Given that object B possesses a greater mass, upon its release, ring A will ascend the rod. When ring A reaches the height of the line that links it to the stationary pulley, it exhibits a rising speed denoted as  $v_1 \neq 0$ . At this moment, let the speed of object B be represented as  $v_2$ . Which of the following is right?



### Options:

- (A)  $v_2 = 0$
- (B)  $v_2 > v_1$
- (C)  $v_2 \neq 0$
- (D)  $v_2 = v_1$

**Ground Truth: (A)**

**o1:**

#### Analysis Approach:

Let the total length of the rope be  $L$ . Divide the rope into two segments: the length from ring A to the fixed pulley is denoted as  $x$ , and the length from the fixed pulley to weight B is denoted as  $y$ . Thus, we have:

$$x + y = L \Rightarrow dx/dt + dy/dt = 0.$$

The problem states that when ring A rises to the horizontal line connecting it to the fixed pulley, "the velocity  $v_1$  of ring A is perpendicular to this segment of the rope (since the rope is horizontal and the ring moves along the vertical rod). Therefore, the rate of change of the rope length due to the ring at this instant is:

$$dx/dt = 0.$$

From the earlier equation  $dx/dt + dy/dt = 0$ , we obtain:

$$dy/dt = 0 \Rightarrow v_2 = 0.$$

This shows that when ring A passes this position, the velocity of weight B is zero.

#### Conclusion:

$$v_2 = 0.$$

Thus, the final answer is:  $\boxed{A}$ .

#### Explanation:

When ring A rises to be parallel with the line connecting to the fixed pulley, in the decomposition of speed  $v_1$ , the speed  $v_{\parallel}$  along the rope direction is the speed  $v_2$  of the weight B. At this moment, the angle  $\theta = 90^\circ$ , which leads to  $\cos\theta = 0$ , therefore  $v_2 = 0$ . Thus, option A is correct, while B, C, and D are incorrect.

#### Explanation-driven analysis: The o1's output is not reasonable.

The model's problem-solving process demonstrates rigorous and self-consistent logic, reflecting genuine comprehension. By analyzing the rate of change in the rope's length, the model correctly deduces that when ring A rises to the horizontal line connecting it to the fixed pulley, the component of ring A's velocity along the direction of the rope is zero, resulting in the velocity  $v_2$  of weight B also being zero. The model employs sound physical analysis and mathematical derivation in its solution, arriving at a conclusion consistent with the standard answer.

The explanation provided by the model further clarifies this reasoning, noting that the  $90^\circ$  angle at this position leads to  $v_2 = 0$ . Thus, the model's solution process is entirely reasonable.

Medium

Illustrations

Physics

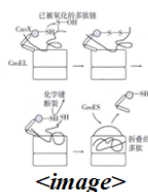
MC

Figure 18: Successful reasoning example of o1.

## Explanation Driven Eval

### Question:

<image> Once a polypeptide chain departs from the ribosome, it requires several minutes for proper folding. Should oxidation occur during this interval, it will influence the folding that follows. Within living cells, the chaperone protein GroEL, along with its cofactor GroES, aids oxidized polypeptide chains in achieving correct conformation. CnoX, a protein that attaches to GroEL, plays a role in this mechanism. The figure illustrates the folding process of a specific polypeptide chain in Escherichia coli. Which of the subsequent analysis is flawed?



### Options:

- (A) The folding of peptide chains is closely related to the amino acid sequence of the composed peptide chains.
- (B) CnoX forms disulfide bonds with the peptide chain, which can prevent the peptide chain from being oxidized.
- (C) GroES and GroEL binding will cause the polypeptide chain to fold.
- (D) CnoX and GroES may have a competitive relationship during their binding process with GroEL.

### Ground Truth: (B)

### QVQ-72B:

A. The folding of the polypeptide chain is closely related to the amino acid sequence that constitutes the polypeptide chain.

This option is correct. The folding of the polypeptide chain is determined by its amino acid sequence, as different amino acids have different side chains that influence the spatial structure of the protein .....

B. The formation of a disulfide bond between CnoX and the polypeptide chain can prevent the polypeptide chain from being oxidized. This option may be **misleading**. First, a disulfide bond (S-S) is formed through the oxidation of the thiol groups (-SH) of two cysteine residues.....

C. The binding of GroES to GroEL induces the folding of the polypeptide chain. This option requires careful consideration. GroEL and GroES are chaperone proteins that assist in the proper folding of proteins. ....

D. There may be a competitive relationship between CnoX and GroES in binding to GroEL. This option is **also plausible**.

**In summary**, options A and C are correct, option B may be misleading, and option D is possibly correct.

However, according to the question's requirements, the incorrect option needs to be identified. It appears that option B may be misleading because the formation of a disulfide bond is actually an oxidative process.....

**To ensure the accuracy of the answer**, I need to analyze the question and options more carefully. First, regarding the folding of polypeptide chains, it is indeed determined by the amino acid sequence, so option A is correct....

**After careful consideration**, I believe option B is likely incorrect because the formation of disulfide bonds is an oxidative process—rather than preventing oxidation, it actually promotes oxidation. Therefore, option B is wrong.

**Final Answer:** `\boxed{B}`.

### Explanation:

The oxidized peptide chain forms a disulfide bond with CnoX, and then the disulfide bond breaks, leading to the reduction of the oxidized peptide chain, so option B is incorrect. The binding of GroES and GroEL triggers the release of CnoX and the folding of the peptide chain, making option C correct. The binding of GroES and GroEL releases CnoX, so it can be inferred that there may be a competitive relationship between CnoX and GroES when binding with GroEL, making option D correct.

### Explanation-driven analysis: The QVQ-72B' s output is reasonable.

The model's problem-solving process is logically rigorous and self-consistent, demonstrating a genuine understanding of the question. The model analyzes each option one by one, particularly the analysis of option B, pointing out that the formation of disulfide bonds is part of the oxidation process rather than a mechanism to prevent oxidation, which aligns with the question's requirement to identify the incorrect option. The model also provides reasonable explanations for the correctness of the other options, especially the analysis of the functions of GroEL and GroES and their relationship with CnoX, showcasing an understanding of biochemical processes.

Therefore, the model's solution is justified.

Medium

Illustrations

Biology

MC

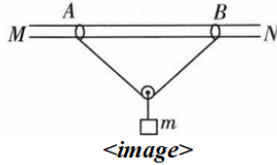
Figure 19: Successful reasoning example of QVQ-72B.



## Explanation Driven Eval

### Question:

<image> Incorporating pull-ups into our regular fitness routines proves to be quite beneficial. Consider a scenario where you hold a horizontal bar with both hands, creating a simplified model: two massless small rings, labeled A and B, are affixed to the horizontal rod MN. An inextensible fine thread connects rings A and B at either end, and a mass  $m$  is suspended from the midpoint of the thread through a small pulley, resulting in an equilibrium state for the entire setup. If the distance between rings A and B is subsequently increased, and the system achieves equilibrium once more, which of the following statements accurately reflects this situation?



### Options:

- (A) Massless small rings A and B both receive increased support.
- (B) Massless small rings A and B both experience reduced friction.
- (C) The tension in the thin line increases.
- (D) The resultant force of small ring A increases.

**Ground Truth: (C)**

### Qwen2.5-VL-72B:

First, consider the situation where the entire system is in equilibrium. Based on the model in the diagram, the weight is stationary, indicating that the tension in the thin string balances the gravitational force  $mg$  of the weight.

Let the angle between the thin string and the horizontal direction be  $\theta$ . According to the equilibrium condition, the tension  $T$  in the string satisfies:  $T \sin \theta = mg/2$ .

This shows that the tension  $T$  is inversely proportional to  $\sin \theta$ . Therefore, when the distance between A and B increases,  $\theta$  decreases, causing  $\sin \theta$  to decrease and consequently the tension  $T$  to increase.

Next, analyze the forces acting on the small rings A and B. Let the normal force exerted by the horizontal rod on the small ring be  $N$ . Since the system is in equilibrium, we have:  $N = T \cos \theta$ .

As  $T$  increases with decreasing  $\theta$ , but  $\cos \theta$  also increases as  $\theta$  decreases, the change in  $N$  depends on the combined effect of  $T$  and  $\cos \theta$ . However, based on the structure of the problem and the analysis of actual physical phenomena, we generally assume that  $N$  does not significantly increase when  $\theta$  decreases. Yet, to make a precise judgment, specific numerical changes would need to be considered. Combining physical intuition and option analysis, it can be inferred that option A in this problem may not hold.

Further analyzing the frictional force  $f$ , we have:  $f = T \sin \theta = mg/2$ .

This indicates that the frictional force  $f$  remains constant once the system reaches stable equilibrium, independent of changes in the string tension or  $\theta$ . Therefore, option B does not hold.

For option D, the net force on the small ring A is always zero because the system is in equilibrium, and there is no scenario where the net force increases. Hence, option D is incorrect.

In conclusion, based on physical analysis and calculations, the tension  $T$  in the string indeed increases.

Thus, the final answer is: \boxed{C}

### Explanation:

When the distance between small rings A and B increases, the angle  $\theta$  between the thin line and MN decreases. In the vertical direction, the balance condition is  $mg = 2T \sin \theta$ . As  $\theta$  decreases,  $\sin \theta$  also decreases, which causes the tension  $T$  to increase, so option C is correct. For the force analysis of small ring A, the horizontal frictional force  $f = T$ . As  $\theta$  decreases,  $\cos \theta$  increases, leading to an increase in  $T$ , so the frictional force on small ring A increases, making option B incorrect. Since A is in a state of equilibrium, the net force remains 0, hence option D is incorrect. The support force  $F_N$  acting on small rings A and B remains unchanged in a state of equilibrium, so option A is incorrect.

### Explanation-driven analysis: The Qwen2.5-VL-72B's output is not reasonable.

The model's problem-solving process is logically rigorous and self-consistent, demonstrating genuine understanding. The model first analyzes the equilibrium state of the system, correctly pointing out that the tension in the thin string balances the gravitational force of the weight. Through mathematical derivation, it concludes that the tension in the string increases as the distance between A and B grows. Next, the model examines the normal forces and frictional forces acting on the small rings A and B, noting that changes in the normal force depend on the combined effect of tension and the angle, while the frictional force remains constant in the equilibrium state. Finally, the model correctly states that the net force on small ring A is always zero because the system is in equilibrium. The entire solution process is clear and reasonable, adhering to fundamental principles of physics and mathematics, ultimately leading to the correct answer, C.

Medium

Illustrations

Physics

MC

Figure 20: Successful reasoning example of Qwen2.5-72B.

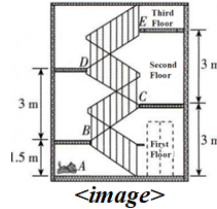




## Explanation Driven Eval

### Question:

<image>In the provided diagram, which illustrates a cross-section of a building, the heights of every floor are indicated. A cat weighing 1kg ascends the stairs starting from point A located on the first floor to reach the third floor. It is established that the gravitational potential energy of the cat at the entrance B of the stairway is zero, while the acceleration due to gravity is specified as  $g=10\text{m/s}^2$ . Which of the subsequent statements is accurate?



### Options:

- (A) The gravitational potential energy of the kitten at point A is 15J
- (B) The gravitational potential energy of the kitten at E is twice that at A.
- (C) The work done by gravity on the kitten from B to D is 30J.
- (D) The potential energy of the kitten increased by 15J as it moved from A to B.

### Ground Truth: (D)

### Claude3.7-sonnet:

I will solve this physics problem, analyzing the changes in gravitational potential energy as the kitten climbs the stairs. First, we need to determine the heights at each point: Point B has a height of 0 (as given in the problem, with B as the reference point for potential energy). Point A is 1.5 m below B, so  $h_A = -1.5\text{m}$ . Point C is 3 m above B, so  $h_C = 3\text{m}$ . Point D is 3 m above C, so  $h_D = 6\text{m}$ . Point E is 3 m above D, so  $h_E = 9\text{m}$ .

Now, let's analyze each option:

A. The gravitational potential energy of the kitten at A is 15 J. Calculating the potential energy at A:

$E_{p,A} = mgh_A = 1 \times 10 \times (-1.5) = -15\text{ J}$ . Thus, option A is incorrect because the potential energy at A is -15J, not 15J.

B. The gravitational potential energy of the kitten at E is twice that at A.

$E_{p,E} = mgh_E = 1 \times 10 \times 9 = 90\text{ J}$ .  $E_{p,A} = -15\text{ J}$ . The ratio is:  $\frac{E_{p,E}}{E_{p,A}} = \frac{90}{-15} = -6$ .

Thus, option B is incorrect because the potential energy at E is not twice that at A.

C. The work done by gravity as the kitten moves from B to D is 30 J.

The work done by gravity equals the decrease in gravitational potential energy:  $W_{\text{gravity}} = E_{p,\text{initial}} - E_{p,\text{final}}$ .

For B to D:  $W_{\text{gravity, B} \rightarrow \text{D}} = E_{p,B} - E_{p,D} = 0 - 60 = -60\text{ J}$ .

Thus, option C is incorrect because the work done by gravity is -60J (meaning the kitten must do 60 J of work against gravity to climb).

D. The gravitational potential energy of the kitten increases by 15 J as it moves from A to B. The change in potential energy is:

$\Delta E_{p,A \rightarrow B} = E_{p,B} - E_{p,A} = 0 - (-15) = 15\text{ J}$ .

Thus, option D is correct—the gravitational potential energy increases by 15 J.

**Final answer:** \boxed{D}

### Explanation:

The gravitational potential energy of the kitten at the bottom of the stairs (B) is 0, so the gravitational potential energy at A is  $E_{p,A} = mgh_A = 1 \times 10 \times 1.5 = 15\text{ J}$ , which makes option A incorrect. The gravitational potential energy of the kitten at E is  $E_{p,E} = mgh_E = 1 \times 10 \times 4.5 = 45\text{ J}$ , thus option B is incorrect. The work done by gravity on the kitten from B to D is  $W_G = -mgh_{BD} = -1 \times 10 \times 3 = -30\text{ J}$ , hence option C is incorrect. The change in gravitational potential energy of the kitten from A to B is  $\Delta E_{p,AB} = mgh_{AB} = 1 \times 10 \times 1.5 = 15\text{ J}$ , which makes option D correct.

### Explanation-driven analysis: The Claude3.7-sonnet's output is not reasonable.

The model's problem-solving process contains inconsistencies and errors. First, when calculating the gravitational potential energy at point E, the model incorrectly used a height of 9 m, whereas the correct height should have been 4.5 m, leading to a discrepancy between the model's calculation and the correct analysis. Second, when computing the work done by gravity from B to D, the model obtained a result of -60 J, while the correct analysis yields -30 J. This inconsistency arises because the model used different height differences (6 m vs. 3 m) in different parts of the solution, resulting in conflicting outcomes. Additionally, the model stated that the work done by gravity was -60 J, whereas the correct value should be -30 J, further demonstrating a lack of coherence in the model's understanding and calculations.

Therefore, the model's reasoning is neither rigorous nor self-consistent, failing to demonstrate a true and accurate understanding of the problem.

Easy

Illustrations

Physics

MC

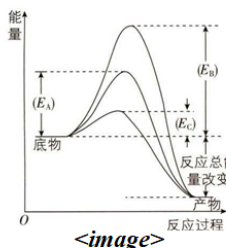
Figure 21: Incorrect reasoning example of Claude3.7-sonnet.



## Explanation Driven Eval

### Question:

<image> Activation energy is defined as the amount of energy necessary for a molecule to shift from its stable state to an active state capable of engaging in chemical reactions. Catalysts function by reducing the activation energy needed for such reactions to occur. The accompanying diagram depicts how both enzymes and inorganic catalysts influence the rate of chemical reactions. Which of the following notations are correct?



### Options:

- (A)  $E_A$  denotes the activation energy for a reaction facilitated by a general catalyst;  $E_B$  signifies the activation energy for a reaction that is not catalyzed; and
- (B)  $E_C$  indicates the activation energy for a reaction that is catalyzed by an enzyme.
- (C) Enzymes have high efficiency, which is essentially due to  $E_B - E_C > E_B - E_A$ .
- (D)  $E_C$  and  $E_A$  represent the activation energies provided by enzymes and inorganic catalysts for chemical reactions, respectively.

Ground Truth: (C)

### Gemini-2.0-flash:

#### Question Analysis:

According to the question, the energy required to transition molecules from their normal state to an active state that facilitates chemical reactions is called the activation energy. The mechanism of a catalyst is to accelerate the reaction by lowering the required activation energy.

In the diagram:

- $E_B$  represents the activation energy of the uncatalyzed reaction,
- $E_A$  represents the activation energy of the reaction catalyzed by an inorganic catalyst,
- $E_C$  represents the activation energy of the enzyme-catalyzed reaction.

#### Option Analysis:

A. Enzymes function as catalysts because they lower the activation energy of chemical reactions, not by providing energy for the reactions. Thus, A is incorrect.

B. The reduction in activation energy by an enzyme is the difference between the activation energy of the enzyme-catalyzed reaction and that of the uncatalyzed reaction. Thus, B is incorrect.

C. The high efficiency of enzymes lies in the fact that they lower the activation energy more significantly than general catalysts, i.e.,  $E_B - E_C > E_B - E_A$ . Thus, C is correct.

D.  $E_C$  and  $E_A$  represent the activation energies of the enzyme-catalyzed and inorganic-catalyzed reactions, respectively, not the activation energy provided for the reactions. Thus, D is incorrect.

Final Answer: \boxed{C}

### Explanation:

Enzymes catalyze reactions by lowering the activation energy required for chemical reactions, so option A is incorrect. According to the figure,  $E_B$  represents the activation energy of the uncatalyzed reaction, and  $E_C$  represents the activation energy of the enzyme-catalyzed reaction. The activation energy lowered by the enzyme is  $E_B - E_C$ , so option B is incorrect. The efficiency of enzymes is evident in their significant effect on lowering activation energy, that is,  $E_B - E_C > E_B - E_A$ , therefore option C is correct.  $E_C$  and  $E_A$  represent the activation energies required for the reaction under enzyme and inorganic catalyst conditions, respectively, so option D is incorrect.

### Explanation-driven analysis: The Gemini-2.0-flash' s output is not reasonable.

There is a logical error in the model's solution, particularly in the analysis of option B. The model incorrectly deemed option B as wrong, when in fact the statement in option B is correct. The statement in option B is "the activation energy reduced by the enzyme is  $E_C$ ," which aligns with the definition given in the question, where  $E_C$  represents the activation energy of the enzyme-catalyzed reaction. In explaining option B, the model confused the activation energy of the enzyme-catalyzed reaction with the activation energy reduced by the enzyme, leading to the erroneous conclusion that option B was incorrect. Aside from this, the model's analysis of option C was correct. However, due to the misunderstanding of option B, the overall solution lacks rigor and self-consistency.

Medium

Charts

Biology

MC

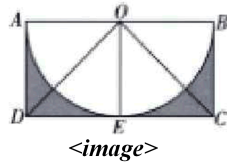
Figure 22: Incorrect reasoning example of Gemini2.0-flash.



## Explanation Driven Eval

### Question:

<image> In the 1630s, Italian mathematician Cavalieri devised a technique for determining the volume of a sphere through the rotation of plane figures, as documented in his work *Geometria indivisibilibus*. The provided figure illustrates that AEB represents a semicircle centered at O, while quadrilateral ABCD acts as the circumscribing rectangle for the semicircle. When this plane figure undergoes a complete rotation around line OE, let the shaded area  $\triangle OCD$  and the semicircle AEB correspond to geometric volumes labeled as  $V_1$ ,  $V_2$ ,  $V_3$ , respectively. Which of the subsequent statements hold true?



### Options:

- (A)  $V_1 + V_2 < V_3$
- (B)  $V_1 + V_2 > V_3$
- (C)  $V_1 > V_2$
- (D)  $V_1 = V_2$

**Ground Truth: (D)**

### InternVL3-78B:

To solve this problem, we need to calculate the volumes of the respective geometric bodies and compare them. First, consider the basic formula for the volume of a solid of revolution:

- When a shape is rotated around a line, the volume of the resulting solid can be calculated using the integral method for solids of revolution. Assume the semicircle AEB has a radius of  $r$ .

1. **Calculate  $V_1$ :**  $V_1$  is half the volume of a sphere formed by rotating the semicircle AEB around the line OE. The volume of a full sphere is:  $V_{\text{sphere}} = \frac{4}{3}\pi r^3$ . Therefore,  $V_1$  is half of the sphere's volume:

$$V_1 = \frac{1}{2} \cdot \frac{4}{3}\pi r^3 = \frac{2}{3}\pi r^3$$

2. **Calculate  $V_2$ :** The shaded  $\triangle OCD$  forms a cone when rotated. The volume of a cone is given by:  $V_{\text{cone}} = \frac{1}{3}\pi r^2 h$ .

Since the length of the rotation axis OE is  $r$ , the height of the cone is  $r$ , and the base radius is also  $r$ :

$$V_{\text{cone}} = \frac{1}{3}\pi r^2 \cdot r = \frac{1}{3}\pi r^3. \text{ Thus, } V_2 = \frac{1}{3}\pi r^3.$$

3. **Calculate  $V_3$ :** The quadrilateral ABCD forms a cylinder when rotated. The volume of a cylinder is:

$$V_{\text{cylinder}} = \pi r^2 h. \text{ Since the rotation axis OE has a length of } r, \text{ the height of the cylinder is } 2r:$$

$$V_{\text{cylinder}} = \pi r^2 \cdot 2r = 2\pi r^3. \text{ Therefore, } V_3 = \pi r^3.$$

**Now, compare  $V_1 + V_2$  and  $V_3$ :**

$$V_1 + V_2 = \frac{2}{3}\pi r^3 + \frac{1}{3}\pi r^3 = \pi r^3. \text{ Thus, the comparison yields: } V_1 + V_2 = \pi r^3 = V_3.$$

From this, we conclude:  $V_1 + V_2 = V_3$

There is no "less than" or "greater than" relationship, so the correct option is:

**The final answer is: \boxed{D}**

### Explanation:

From the concept of a rotating body, we know that the geometric bodies formed by the rotation of  $\triangle OCD$ , the shaded area, and the semicircle AEB are a cone, a cylinder minus a hemisphere of the same radius, and a hemisphere, respectively. Let  $OE = DE = r$ , then  $V_1 = \frac{1}{3}\pi r^2 \cdot 2r = \frac{2}{3}\pi r^3$ ,  $V_2 = \pi r^2 \cdot r = \pi r^3$ ,  $V_3 = \frac{1}{2} \cdot \frac{4}{3}\pi r^3 = \frac{2}{3}\pi r^3$ . Therefore,  $V_1 = V_2$ , and  $V_1 + V_2 = V_3$ , so the answer is D.

### Explanation-driven analysis: The InternVL3-78B's output is not reasonable.

The model's problem-solving process contains logical errors and inconsistencies. First, in the solution, when calculating  $V_1$ , the model correctly interprets  $V_1$  as half the volume of the sphere formed by rotating the semicircle AEB around the line OE. However, when calculating  $V_2$ , the model mistakenly treats the geometric body formed by rotating the shaded triangle ( $\triangle OCD$ ) as a cone and incorrectly assumes its height and base radius are both  $r$ . In reality, the geometric body formed by rotating ( $\triangle OCD$ ) is a cone, but its height should be the length of OE, and its base radius should be the length of OD.

Additionally, the formulas for calculating  $V_1$  and  $V_2$  in the explanation are inconsistent with those in the solution. Moreover, the results for  $V_1$  and  $V_2$  in the explanation are the opposite of those in the solution. Finally, the model's conclusion that  $V_1 + V_2 = V_3$  does not align with the calculations provided in the solution.

Therefore, the model's problem-solving process lacks rigor and self-consistency.

Medium

Geometric  
Shapes

Math

MC

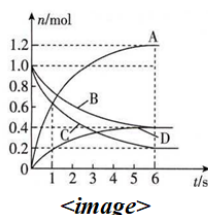
Figure 23: Incorrect reasoning example of InternVL3-78B.



## Explanation Driven Eval

### Question:

Two gases are placed in a sealed container with a volume of 4L at a specific temperature to participate in a reversible reaction. The alterations in the quantities of substances throughout the reaction are illustrated in the accompanying figure. Based on this information, which inference regarding the reaction can be considered reasonable?



### Options:

- (A) The chemical equation for the reaction is  $3B + 4C \rightleftharpoons 6A + 3D$
- (B)  $0 \sim 1s$ ,  $v(A) = v(D)$ .
- (C)  $0 \sim 6s$ , the reaction rates of all substances are equal.
- (D) The average reaction rate of B from  $0 \sim 6s$  is  $0.025 \text{ mol} \cdot \text{L}^{-1} \cdot \text{s}^{-1}$ .

Ground Truth: (D)

### o1:

#### Analysis and Solution:

First, estimate the amounts of each substance (in mol) at  $t = 0$  and  $t = 6s$  from the graph. The following values are approximate (refer to the given figure for accuracy): B decreases from about 1.0mol to about 0.4mol, so  $\Delta n_B \approx -0.6\text{mol}$ . The container volume  $V = 4L$ , and the total reaction time  $\Delta t = 6s$ . If option D states "the average reaction rate of B from 0 to 6s is  $0.025 \text{ mol} \cdot \text{L}^{-1} \cdot \text{s}^{-1}$ ", we can first calculate the average reaction rate of B during this period (taking the consumption rate as positive):

$$v_{\text{avg}}(B) = -\Delta n_B / (V \cdot \Delta t) = -(-0.6\text{mol}) / (4L \cdot 6s) = 0.6/24 = 0.025 \text{ mol} \cdot \text{L}^{-1} \cdot \text{s}^{-1}.$$

This matches the data estimated from the graph, so option D is consistent.

Now, examine the other options:

1. Option A gives the chemical equation  $3B + 4C \rightleftharpoons 6A + 3D$ , which implies a stoichiometric ratio of  $-n_B : -n_C : +n_A : +n_D = 3 : 4 : 6 : 3$ . However, the estimated changes in the amounts of the substances from the graph do not satisfy this ratio. Thus, A is unreasonable.
2. Option B claims that  $v(A) = v(D)$  in the time interval 0 to 1s. If their stoichiometric coefficients are not equal or their slopes in the graph are not identical, this cannot hold. Therefore, B is unreasonable.
3. Option C states that the reaction rates of all substances are equal from 0 to 6s. However, the actual generation or consumption rates of different substances must be divided by their respective stoichiometric coefficients to be equal. Moreover, the graph shows that their slopes vary over time, so C is also unreasonable.

In conclusion, only option D aligns with the given data and calculations.

Thus, the final answer is:  $\boxed{D}$ .

### Explanation:

From the title image, we can see that when the reaction reaches equilibrium, the amount of substance A increases by 1.2mol, the amount of substance D increases by 0.4mol, the amount of substance B decreases by 0.6mol, and the amount of substance C decreases by 0.8mol. Therefore, A and D are the products, while B and C are the reactants. The ratio of the changes in the amounts of substances B, C, A, and D is 3:4:6:2, so the chemical equation is  $3B + 4C \rightleftharpoons 6A + 2D$ . Thus, option A is incorrect; the ratio of the reaction rates is equal to the ratio of the stoichiometric coefficients, so  $0 \sim 1s$ ,  $v(A) = 3v(D)$ , making option B incorrect; according to the stoichiometric coefficients of the reaction, the reaction rates of the substances are not equal, hence option C is incorrect; for  $0 \sim 6s$ , the change in the amount of substance B is 0.6 mol, and the volume of the container is 4L, so  $v(B) = \Delta c / \Delta t = 0.6/6 = 0.1 \text{ mol} \cdot \text{L}^{-1} \cdot \text{s}^{-1}$ . Therefore, option D is correct.

### Explanation-driven analysis: The o1' s output is not reasonable.

The problem-solving process of the model contains logical errors, particularly in calculating the average reaction rate for option D. The model computed the average reaction rate as  $0.025 \text{ mol} \cdot \text{L}^{-1} \cdot \text{s}^{-1}$ , whereas the Chinese analysis indicated the correct calculation should yield  $0.1 \text{ mol} \cdot \text{L}^{-1} \cdot \text{s}^{-1}$ . This suggests that the model may have made a mistake or misinterpretation during the calculation.

Additionally, the model's reasoning when analyzing options A, B, and C was not rigorous enough, failing to accurately explain the relationship between stoichiometric coefficients and reaction rates. As a result, the model's problem-solving process does not demonstrate a genuine understanding of the question but rather arrived at the correct answer by coincidence.

Easy

Charts

Chemistry

MC

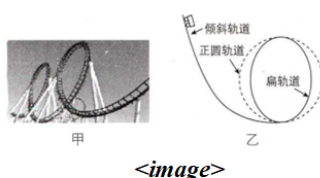
Figure 24: Incorrect reasoning example of o1.



## Explanation Driven Eval

### Question:

*<image>* Typically, the vertical loop tracks of roller coasters do not form perfect circles; instead, they exhibit a flattened design that is taller in the vertical direction and more constrained in the horizontal span, as illustrated in Figure A. In Figure B, a basic schematic representation is provided, where a small car (treated as a point mass) is let go from rest at a specific elevation on an inclined track, ignoring all forms of resistance. Upon reaching the apex of the flattened track, how does this height compare to that of a circular track positioned at the same elevation?



### Options:

- (A) On a flat track, the cart experiences greater centripetal force and exerts more pressure on the track.
- (B) On the flat track, the cart moves at a higher speed, putting more pressure on the track.
- (C) On the flat track, the cart has a smaller acceleration, resulting in less pressure on the track.
- (D) The mechanical energy of the cart on the flat track is smaller, resulting in less pressure on the track.

Ground Truth: (A)

### QVQ-72B:

Alright, this problem is about the vertical loop of a roller coaster. The question states that many roller coasters' vertical loop tracks are not perfect circles but are instead flattened structures that are taller vertically and narrower horizontally. As shown in Figure A, there's an actual photo of a roller coaster track, and Figure B is a simplified diagram of this structure, which includes an inclined track, a perfectly circular track, and a flattened track.

The question says: A small car (which can be treated as a particle) is released from rest at a certain height on the inclined track, and all resistances are ignored. When the car reaches the highest point of the flattened track, how does it compare to the highest point of a perfectly circular track at the same height?

....

However, a more detailed analysis might be needed here. ....

So, perhaps my understanding is incorrect.

It might be necessary to consider the normal force from the track.

At the highest point, the car is subject to gravity and the normal force from the track, and their resultant provides the centripetal force. ....

So, based on the given options, I might need to choose the one that is closest to being correct, which is option A. Although it states that the pressure on the track is greater—which may not be entirely accurate—it is likely the most plausible answer.

However, I'm not entirely sure about this.

Thus, I ultimately choose option A, though I have some doubts.

Final Answer: \boxed{A}

### Explanation:

From the release point to the highest point, according to the work-energy theorem, we have  $mg\Delta h = \frac{1}{2}mv^2$ . Since the highest points of the flat track and the circular track are the same, the speed at the highest point is also the same. The radius of the flat track is smaller than that of the circular track. According to the centripetal force formula  $F_n = \frac{mv^2}{r}$ , it can be concluded that the centripetal force on the flat track is greater, and the centripetal acceleration is also greater. Therefore, the support force from the track on the cart is larger. As a result, the pressure the cart exerts on the track is also greater, making option A correct. Since we ignore all forms of resistance, the mechanical energy of the cart on the flat track is the same as that on the circular track, thus option D is incorrect.

### Explanation-driven analysis: The QVQ-72B's output is not reasonable.

The problem-solving process in the model contains logical inconsistencies and misunderstandings. First, the model contradicts itself in the analysis, particularly when discussing the relationship between speed and centripetal force. It mentions that "the speed might be the same due to energy conservation," but elsewhere suggests that "the speed could be greater on the flattened track," indicating a lack of clarity in understanding the connection between energy conservation and velocity. Additionally, the model incorrectly assumes that the normal force (support force) could be negative, which is physically unreasonable since the normal force represents the track's reaction force on the car and cannot be negative.

Finally, the model displays uncertainty in selecting the answer, ultimately choosing option A seemingly based on guesswork rather than rigorous reasoning. Although the final answer matches the correct one, the model's problem-solving process lacks a clear and logical chain of reasoning.

Medium

Photos,  
Illustrations

Physics

MC

Figure 25: Incorrect reasoning of of QVQ-72B.

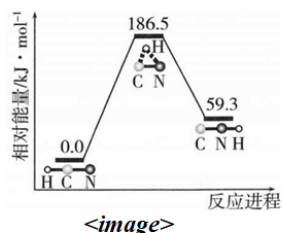




## Explanation Driven Eval

### Question:

According to theoretical studies, the figure illustrates the energy change associated with the isomerization reaction  $\text{HCN}(\text{g}) \rightleftharpoons \text{HNC}(\text{g})$  at 101 kPa and 298 K. Identify the statement among the following options that is false.



### Options:

- (A) HCN is more stable than HNC.
- (B) The value of the isomerization reaction is  $\Delta H = +59.3 \text{ kJ} \cdot \text{mol}^{-1}$
- (C) The activation energy for the forward reaction is greater than that for the reverse reaction.
- (D) Using a catalyst can change the reaction's enthalpy

Ground Truth: (D)

### Qwen2.5-VL-72B:

To solve this chemistry problem, we need to analyze the reaction pathway diagram and the reaction principles.

**Option A:** HCN is more stable than HNC

According to the diagram, the relative energy of HCN (initial state) under the conditions of 101 kPa and 298 K is  $0.0 \text{ kJ} \cdot \text{mol}^{-1}$ , while the relative energy of HNC (product) is  $+59.3 \text{ kJ} \cdot \text{mol}^{-1}$ . Since substances with lower energy are more stable, HCN is more stable than HNC. Therefore, Option A is correct.

**Option B:** The enthalpy change of this isomerization reaction is  $\Delta H = +59.3 \text{ kJ} \cdot \text{mol}^{-1}$

The reaction enthalpy  $\Delta H$  can be directly obtained from the energy difference between the initial and final states in the diagram. The energy difference between the initial state (HCN) and the final state (HNC) is  $+59.3 \text{ kJ} \cdot \text{mol}^{-1}$ . Thus, by definition, Option B is also correct.

**Option C:** The activation energy of the forward reaction is greater than that of the reverse reaction

From the energy curve in the diagram, the activation energy of the forward reaction is the energy difference from  $0.0 \text{ kJ} \cdot \text{mol}^{-1}$  to  $186.5 \text{ kJ} \cdot \text{mol}^{-1}$ , which is  $186.5 \text{ kJ} \cdot \text{mol}^{-1}$ . The activation energy of the reverse reaction is the energy difference from  $59.3 \text{ kJ} \cdot \text{mol}^{-1}$  back to  $0.0 \text{ kJ} \cdot \text{mol}^{-1}$ , which is  $59.3 \text{ kJ} \cdot \text{mol}^{-1}$ . Therefore, we can conclude that the activation energy of the forward reaction  $E_{a,\text{forward}} = 186.5 \text{ kJ} \cdot \text{mol}^{-1} > E_{a,\text{reverse}} = 59.3 \text{ kJ} \cdot \text{mol}^{-1}$ , so Option C is correct.

**Option D:** Using a catalyst can change the reaction enthalpy

Catalysts only alter the reaction pathway, lowering the activation energy and thereby accelerating the reaction rate. However, they do not change the energy levels of the reactants and products, so the reaction enthalpy  $\Delta H$  remains unchanged. Therefore, Option D is incorrect.

In summary, the incorrect option is D.

The final answer is: \boxed{D}

### Explanation:

The lower the material energy, the more stable it is; therefore, HCN is more stable than HNC. This isomerization reaction is an endothermic reaction, where the total energy of the reactants is lower than the total energy of the products, and  $\Delta H = +59.3 \text{ kJ} \cdot \text{mol}^{-1}$  is correct. According to the diagram, the activation energy for the forward reaction is  $186.5 \text{ kJ} \cdot \text{mol}^{-1}$ , while the activation energy for the reverse reaction is  $127.2 \text{ kJ} \cdot \text{mol}^{-1}$ , so the activation energy for the forward reaction is greater than that for the reverse reaction. A catalyst can lower the activation energy of the reaction but does not change the reaction's heat, so option D is incorrect.

### Explanation-driven analysis: The Qwen2.5-VL-72B's output is not reasonable.

The model's explanation contains an error in the analysis of option C. The model's solution states that the activation energy of the reverse reaction decreases from  $59.3 \text{ kJ} \cdot \text{mol}^{-1}$  back to  $0.0 \text{ kJ} \cdot \text{mol}^{-1}$ , i.e.,  $59.3 \text{ kJ} \cdot \text{mol}^{-1}$ , which is clearly incorrect. According to the diagram, the activation energy of the reverse reaction should be from  $59.3 \text{ kJ} \cdot \text{mol}^{-1}$  to  $186.5 \text{ kJ} \cdot \text{mol}^{-1}$ , i.e.,  $127.2 \text{ kJ} \cdot \text{mol}^{-1}$ . The explanation correctly points this out, but the solution does not reflect a proper understanding of the reverse reaction's activation energy. Therefore, although the final answer is correct, the model's problem-solving process is not rigorous or self-consistent.

Medium

Charts

Chemistry

MC

Figure 26: Incorrect reasoning example of Qwen2.5-72B.